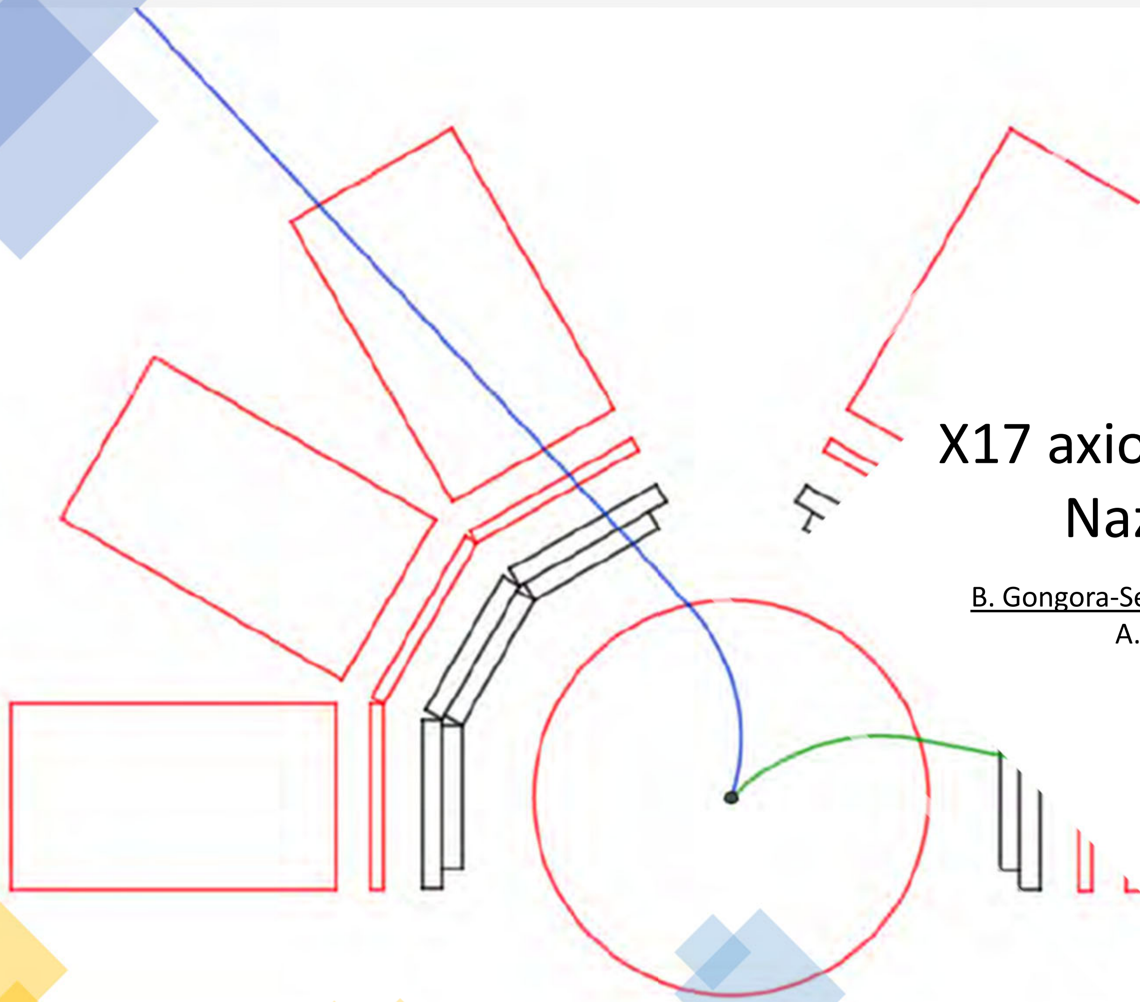

X17 axion search at Laboratori Nazionali di Legnaro

B. Gongora-Servin, **T. Marchi**, D. Tagnani, A. Celentano, A. Goasduff, J.J. Valiente-Dobón

and the NUCLEX collaboration

Krakow 19/09/2023

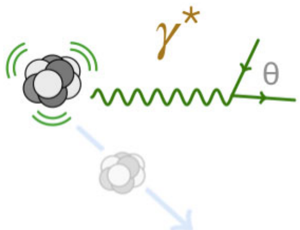

Emission of e^+e^- pairs coupled to the Nuclear Field.
It must be disentangled from pair production due to high energy gamma rays.

- Possible only for ΔE>1.022 MeV
- Competes with gamma emission (typical cross section ratio is 10^{-3})
- Allowed for monopole transitions
- Allows to directly probe transition properties

Theory is well established since Rose's work:

- M.E. Rose, Phys Rev 76, 678 (1949);
- E.K. Warburton, Phys Rev 133, 6B (1964)
- P. Schlüter et al, Phys Rep 75, 327 (1981)
- P. Schlüter et al, At Data and Nucl Data Tab 24, 509 (1979)

It is possible to compute:

Pair Conversion Coefficients (PCC)

Electron-positron angular correlations

Detecting "high energy" e+e- pairs (sharing 10-20 MeV of kinetic energy) emitted in an environment dominated by gamma-rays poses an experimental challenge.

Outline

- Motivation and interest on the "X17 case"
- Aipac8Be: a new setup at LNL for IPC studies
- Performance evaluation – experimental results

Motivation: renewed interest on IPC.

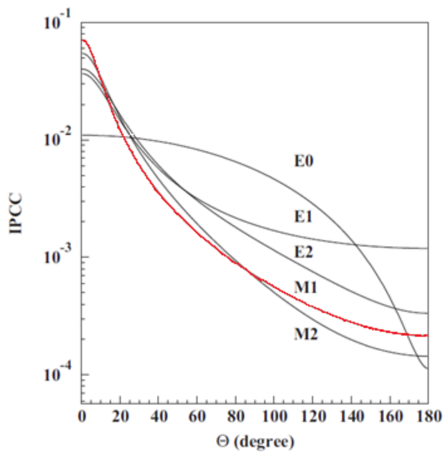

A. J. Krasznahorkay et al. (2016)

Beam: protons in the 0.5 -1.2 MeV range

Targets: LiF_2, LiO_2.

The reaction: $^{7}Li(p,e^{+}e^{-})^{8}Be$ allows to selectively populate the 17.64 MeV and 18.15 MeV resonances.

The considered transitions are M1 type. Isospin is assigned in analogy to isobaric nuclei -> two iso-scalar and two iso-vector transitions.

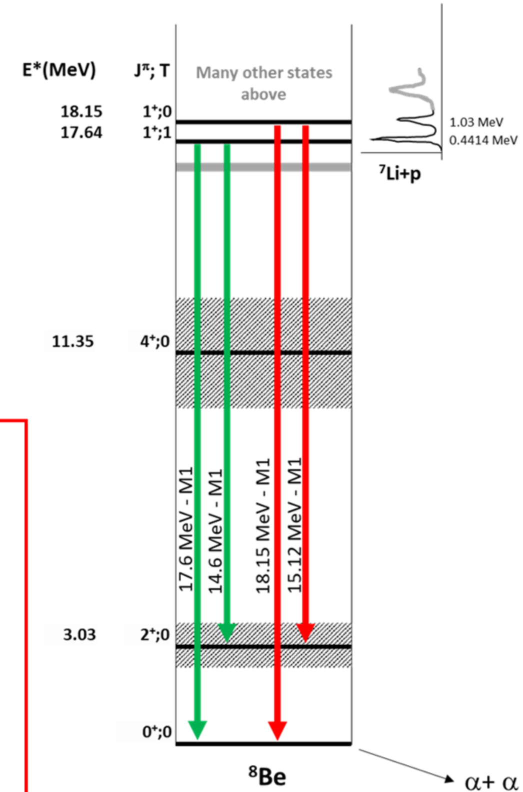

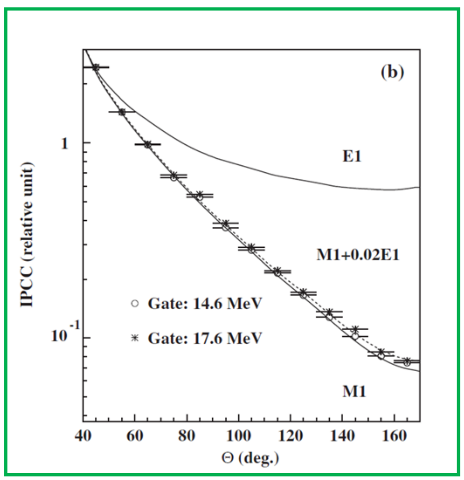

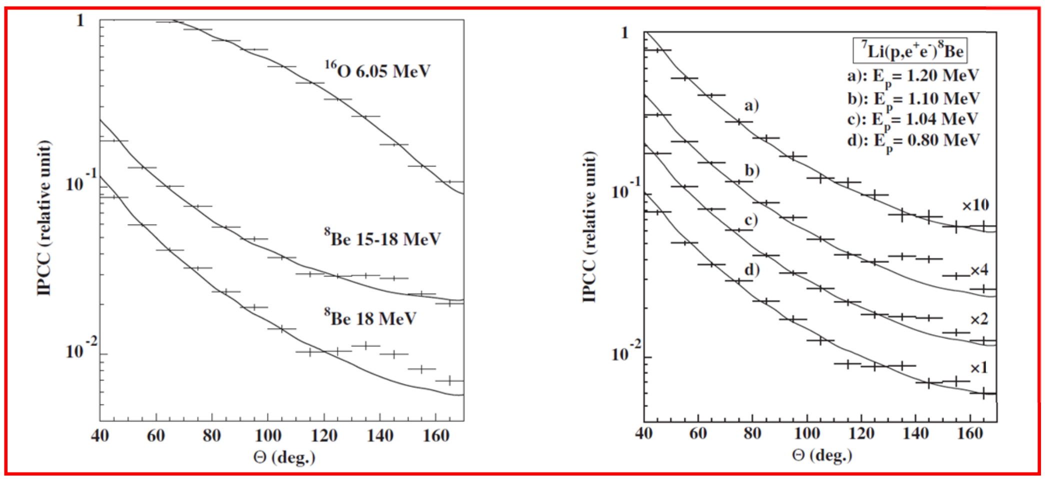

[A. J. Krasznahorkay et al, Phys Rev Lett 116, 042501 (2016)]

Motivation: curiosity for the “X17” case.

PRL **116,** 042501 (2016) PHYSICAL REVIEW LETTERS week ending 29 JANUARY 2016

Observation of Anomalous Internal Pair Creation in ^{8}Be: A Possible Indication of a Light, Neutral Boson

A. J. Krasznahorkay,* M. Csatlós, L. Csige, Z. Gácsi, J. Gulyás, M. Hunyadi, I. Kuti, B. M. Nyakó, L. Stuhl, J. Timár,

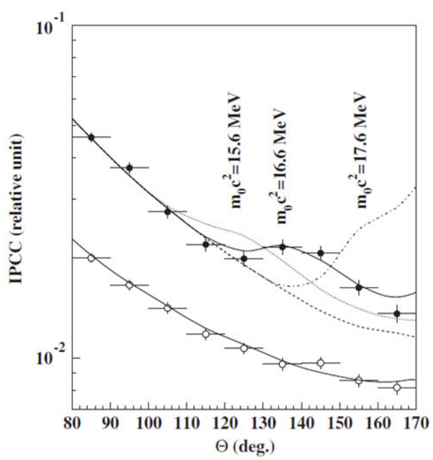

FIG. 4. Experimental angular e^+e^- pair correlations measured in the $^{7}\mathrm{Li}(p, e^+e^-)$ reaction at $E_p = 1.10$ MeV with $-0.5 \le y \le 0.5$ (closed circles) and $|y| \ge 0.5$ (open circles). The results of simulations of boson decay pairs added to those of IPC pairs are shown for different boson masses as described in the text.

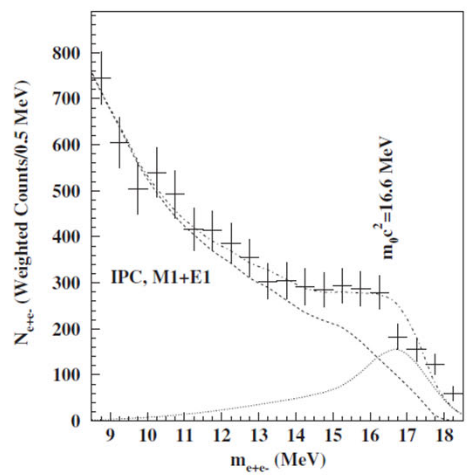

FIG. 5. Invariant mass distribution derived for the 18.15 MeV transition in ^{8}Be.

The deviation between the experimental and theoretical angular correlations is significant and can be described by assuming the creation and subsequent decay of a $J^{\pi}=1^{+}$ boson with m_0c^2=16.70±0.35(stat)±0.5(syst) MeV/c^2. The branching ratio of the e^+e^- decay of such a boson to the γ-decay of the 18.15 MeV level of ^{8}Be was found to be 5.8×10^{-6} for the best fit.

Such a boson might be a good candidate for the relatively light $U(1)_d$ gauge boson [4], or the light mediator of the secluded WIMP dark matter scenario [5] or the dark Z (Zd) suggested for explaining the muon anomalous magnetic moment [7].

Literature on IPC anomaly.

F.W. N. de Boer et al, Phys Lett B 388, 235 (1996)
F.W. N. de Boer et al, J. Phys G: Nucl Part Phys 23, L85 (1997)
F.W. N. de Boer et al, J Phys G: Nucl Part Phys 27, L29 (2001)
And several others.

Results of two dedicated experiments are reported yielding further indications for an anomaly at 9 MeV/c2 in the angular correlation of IPC. The first experiment (8Be) shows a deviation from IPC at large correlation angles presumably due to the same anomaly in the transition to the first excited state. The second experiment (12C) shows a relatively large anomaly at 9 MeV/c2, albeit with limited statistics. Both results are compatible with an X-boson scenario where the boson–nucleon coupling strength is proportional to the isoscalar strength in the M1 transition. Exploiting isospin structure as a guideline, further high statistics experiments are needed to establish the nature of the anomaly.

Table 1. Experimental results relevant for the search of anomalous e^+e^- production in nuclear transitions with respect to IPC, in the invariant mass range from 5 to 15 MeV/c^2. Listed are the nucleus, the quantum numbers, the energy (E) and character (E1, M1) of the transition, the derived boson emission branching ratio (B_X) with respect to γ emission, the boson decay width (Γ_X), the isospin dependent effective coupling strength (α_X), relative to $\tilde{\alpha} = 1.7 \times 10^{-6}$ (the axion–nucleon coupling strength), the invariant mass m_X and the literature references. Values for B_X and Γ_X have been derived at 95% CL.

^AZ	I^π	T	E MeV	B_X	Γ_X meV	α_X 1.7×10^{-6}	m_X MeV/c^2	Reference
^{20}Ne	1^-	1	17.8 E1	$\leqslant 1.3 \times 10^{-4}$	$\leqslant 3$	$\leqslant 1.8$		[20]
			16.2 E1					
^{12}C	1^-	1	17.2 E1	$\leqslant 2.3 \times 10^{-5}$	$\leqslant 1$	$\leqslant 0.3$		[1]
	2^-	1	12.3 E1					
^{12}C	1^+	0	12.7 M1	$(1.6 \pm 0.7) \times 10^{-3}$	0.55 ± 0.24	38 ± 17	9.2 ± 1.0	[6]
^{12}C	1^+	1	15.1 M1	$\leqslant 4.6 \times 10^{-5}$	$\leqslant 1.7$	$\leqslant 0.9$		[6]
^{12}C			114 M1	$\leqslant 9.8 \times 10^{-5}$	$\leqslant 8$	$\leqslant 0.8$		[8, 23]
^{8}Be	1^+	1, 0	17.6 M1	$(11.4 \pm 3.4) \times 10^{-5}$	1.9 ± 0.4	1.5 ± 0.4	9 ± 1	[1]
			14.6 M1					
^{4}He	0^-	0	21.0 e^+e^-		74 ± 30	32 ± 12	8 ± 2	[15, 5]

Table 1. Experimental results for anomalous e^+e^--emission interpreted in the light of a short-lived 9 MeV/c^2 X-boson in six M1 transitions and an M0 transition. Listed are the nucleus, the energy and the width of the resonance E_R and Γ_R, the (iso)spin-parity quantum numbers, the transition energy E_γ, the X-branching ratio B_X with respect to γ-emission, the X-decay width Γ_X, the coupling strength α_X relative to $\tilde{\alpha} = 1.7 \times 10^{-6}$ (the axion–nucleon coupling strength), the invariant mass m_X, and the references. Values for B_X and m_X have been derived at 95% CL.

^AZ	E_R (MeV)	Γ_R (eV)	I^π, T	E_γ (MeV)	B_X	Γ_X (meV)	α_X 1.7×10^{-6}	m_X (MeV/c^2)	Refs
^{12}C	12.71	18.1	$1^+, 0$	12.71	$(7 \pm 3) \times 10^{-4}$	0.24 ± 0.11	18 ± 7	9.0 ± 1.0	Present
				12.71	$(1.6 \pm 0.7) \times 10^{-3}$	0.56 ± 0.25	38 ± 17	9.2 ± 1.0	[5–7]
	15.11	43.6	$1^+, 1$	15.11	$\leqslant 4.6 \times 10^{-5}$	$\leqslant 1.8$	$\leqslant 0.9$	—	[5–7]
^{8}Be	17.64	10.7×10^3	$1^+, 1$	17.64	$(1.1 \pm 0.3) \times 10^{-4}$	1.9 ± 0.4	1.5 ± 0.4	9 ± 1	[2–4]
				14.64	$(8.5 \pm 2.6) \times 10^{-5}$	0.7 ± 0.2	1.5 ± 0.4	9 ± 1	[2–4]
	18.15	138×10^3	$1^+, 0$	18.15	$\leqslant 4.1 \times 10^{-4}$	$\leqslant 1.2$	$\leqslant 5.7$	—	Present
				15.15	$(5.8 \pm 2.2) \times 10^{-4}$	2.2 ± 0.8	10.5 ± 4.5	9.5 ± 1.2	Present
^{4}He	21.0	850×10^3	$0^-, 0$	M0	$0^- \to 0^+, e^+e^-$	74 ± 30	32 ± 12	8 ± 2	[5–7]

Is alpha-clustering hiding behind the scene?

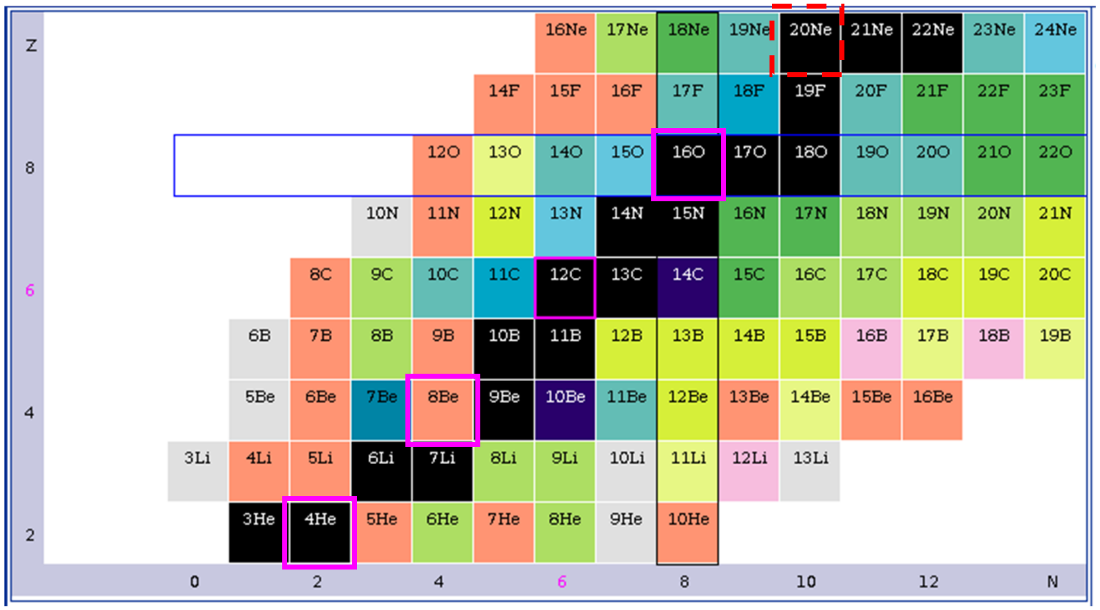

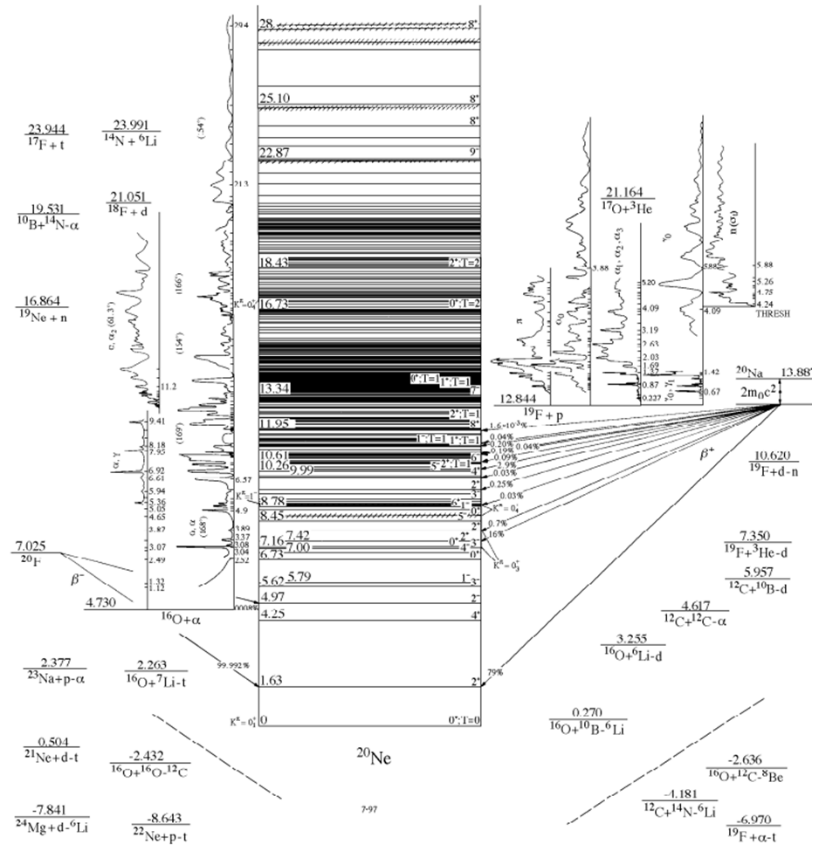

Setups used for pair spectroscopy

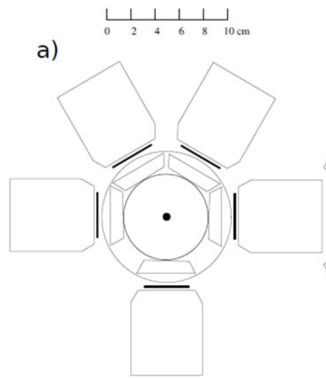

Figure 1. Comparison between the old and new setups. The previous setup (a) used 5 telescopes, each with a MWPC to gather the position of the particles and a thin scintillator in front of the main one to differentiate electrons and positrons from gammas. The new setup (b) consisted of 6 telescopes, and the MWPCs was replaced by DSSDs, which can be used for the particle identification, removing the need for the thin scintillators.

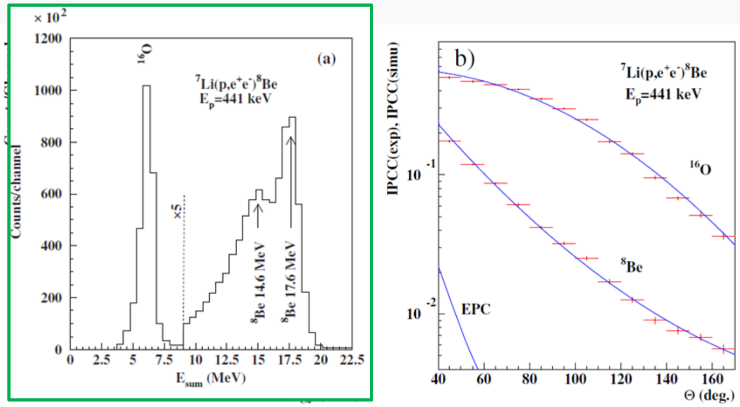

Figure 2. Energy sum spectrum (a) and angular correlation (b) of the $e^{+}e^{-}$pairs from the 17.6 MeV transition. Full blue curve shows the simulated results, and red points with error bars shows the experimental results

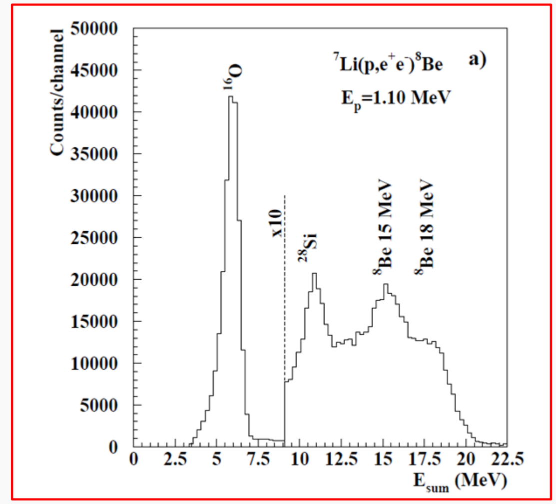

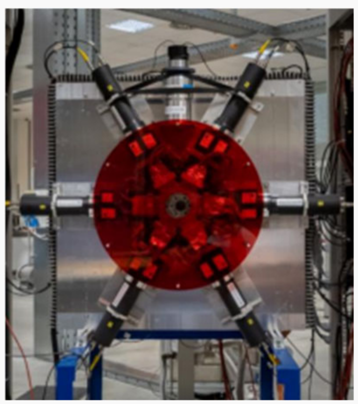

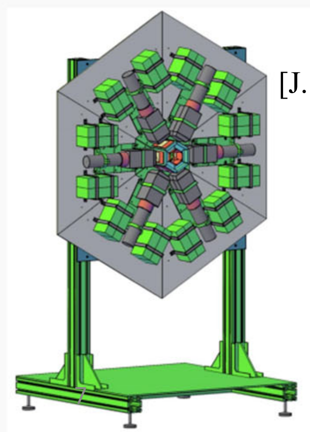

[D. S. Firak et al, EPJ Web of Conferences 232, 04005 (2020)]

[J. Gulyás et al, Nucl Instr and Meth in Phys Res A 808, 21 (2016)]

[A. J. Krasznahorkay et al, arXiv:1504.01527]

Can we provide independent data?

We do have a useful facility

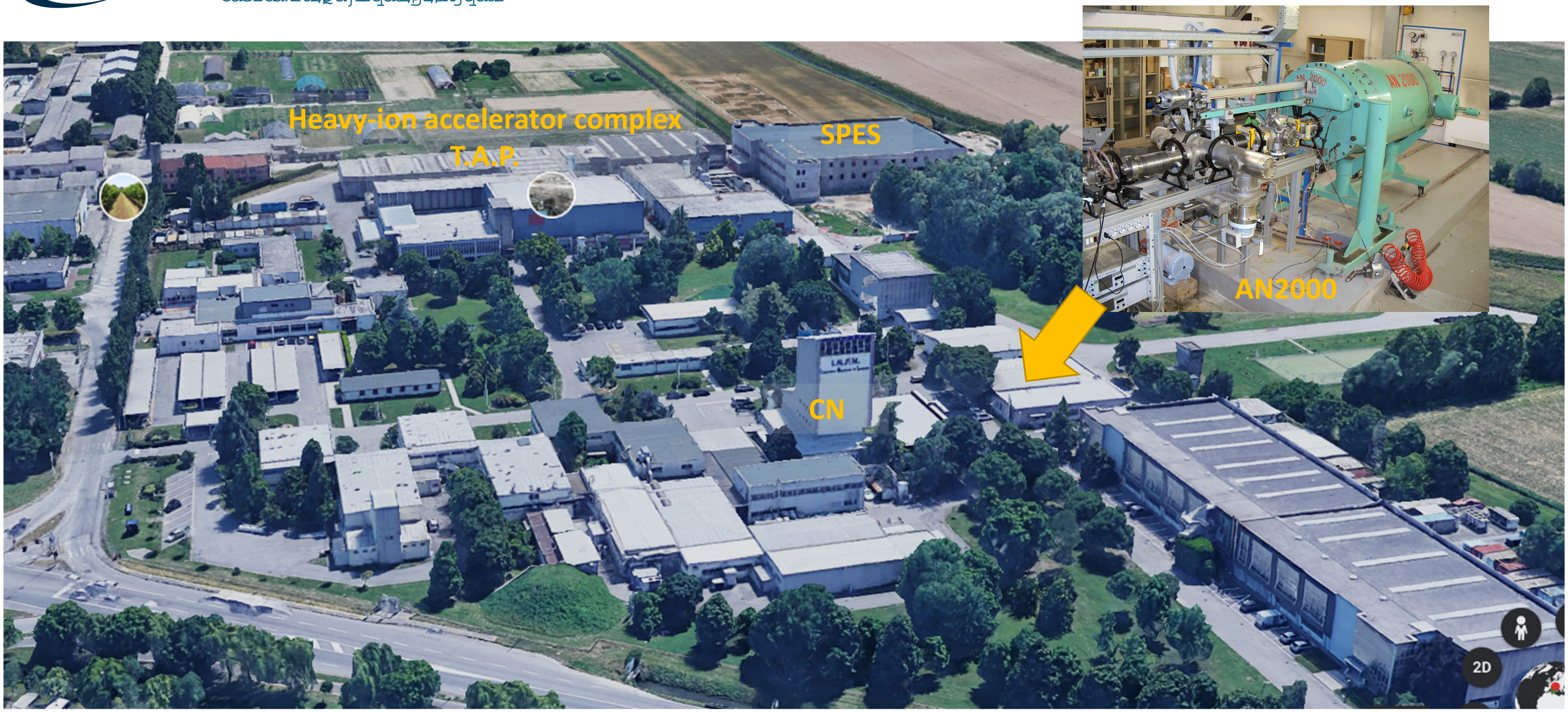

AN2000 by High Voltage Engineering
Operational since 1971.

Ions: $^{1\,(2)}$H+, $^{3\text{-}4}$He+.
Maximum Terminal Voltage: 2.5 MV, single stage (belt).
Beam current: up to 1 μA.

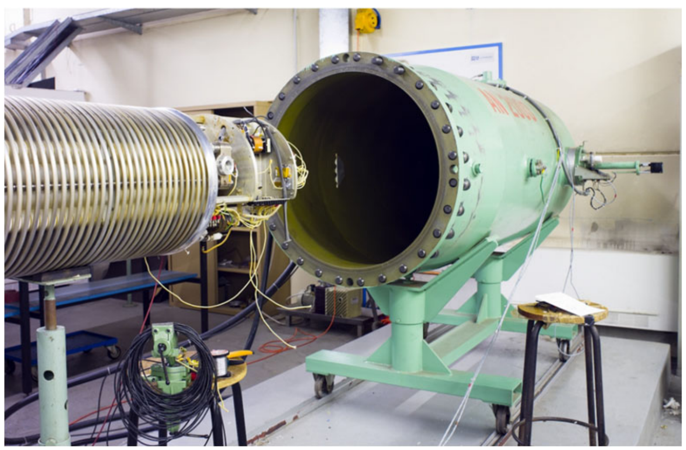

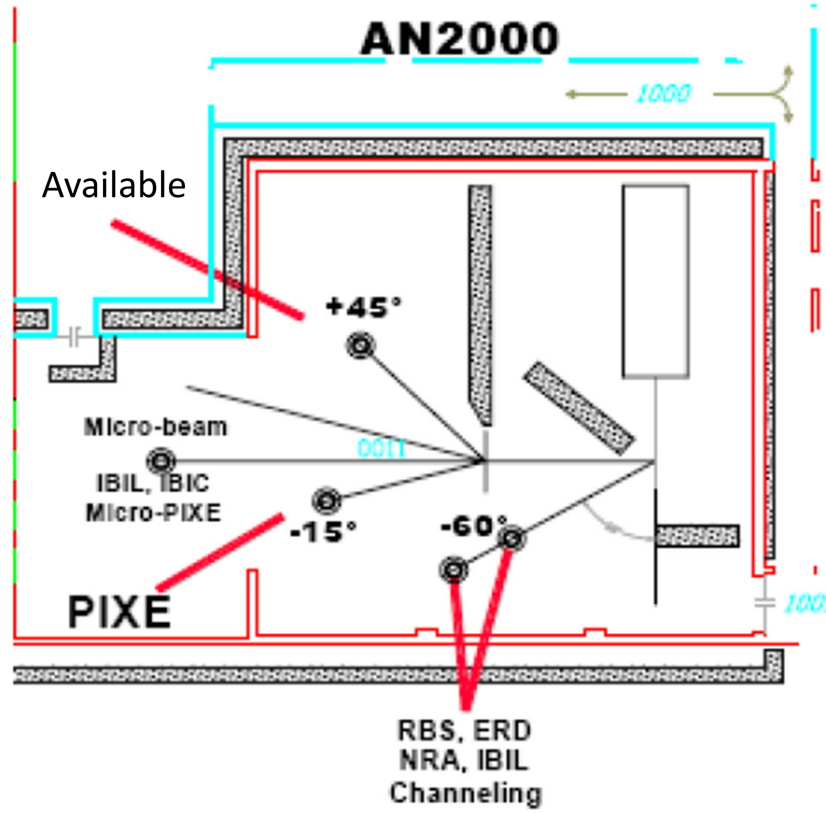

[https://www.lnl.infn.it/index.php/en/home-3/9-uncategorised/235-featuresbeams]

Design of a new IPC setup: can we improve sensitivity?

- Positrons are not discriminated from electrons. -> Future coupling to magnetic field.
- Target composition and stability are critical.
- Solid angle coverage is limited to theta=90°.
- Can we improve energy resolution?
- Angular resolution is limited by straggling:

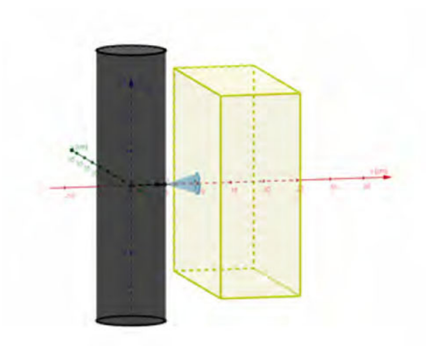

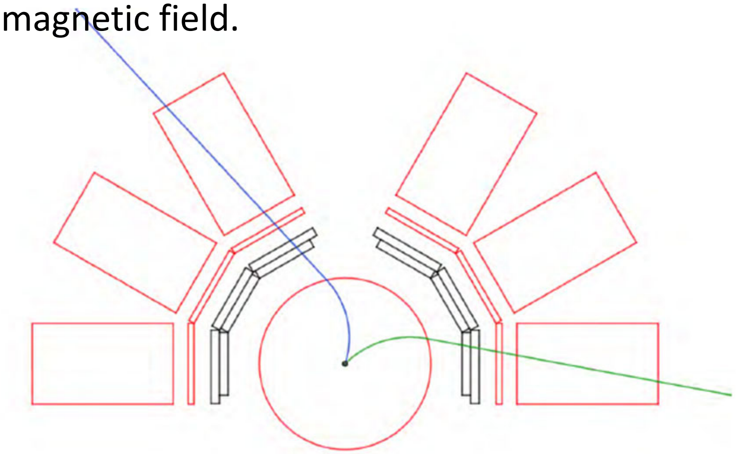

Spessore [mm]	Energie [MeV]		
	10	15	20
0.7	8°	5.5°	3.5°
1	9°	6.8°	4.5°
1.5	11°	8°	5.5°

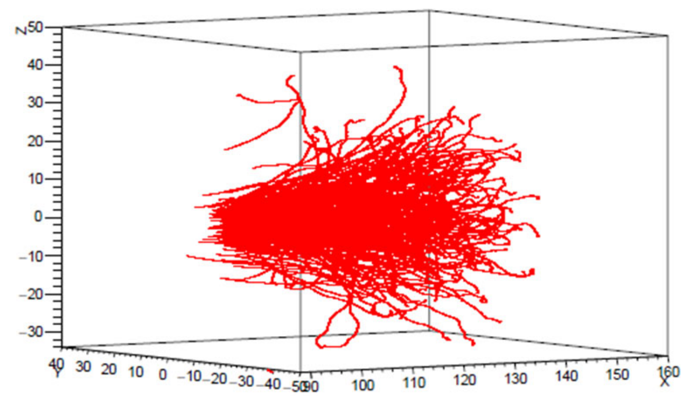

[R. Bolzonella, Preparazione di un esperimento per la misura di coppie e+e- nel decadimento del 8Be*, Università di Padova (2019)]

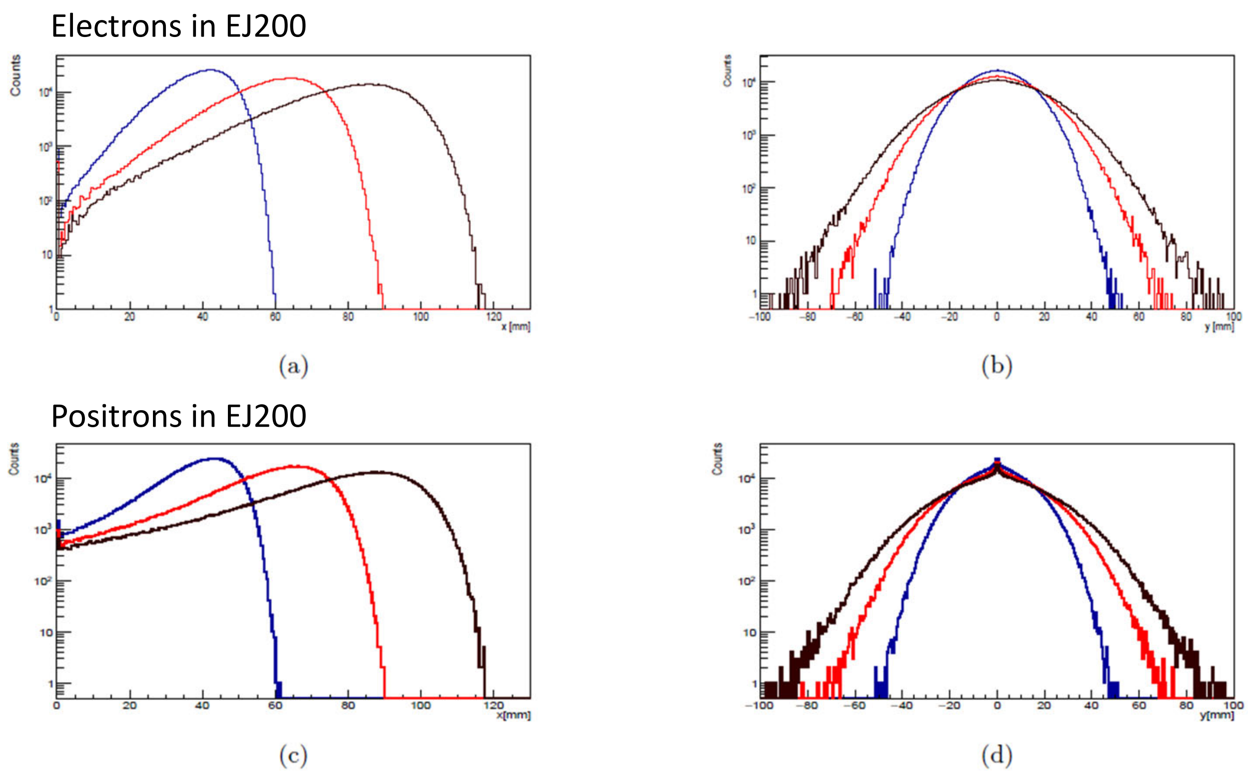

Figure 3.1: Absorption position of electrons (**a**, **b**) and positrons (**c**, **d**), with a logarithmic scale on the counts, at different emission energies: 10 MeV (blue), 15 MeV (red), 20 MeV (brown).

A new setup: proposal

- Improve angular resolution by reducing material budget.
- Improve angular coverage and measure out-of-plane correlation
- Improve confidence on target composition.

- Allow future coupling with a magnetic field.

- Focus on ^{8}Be and, possibly, ^{12}C cases.

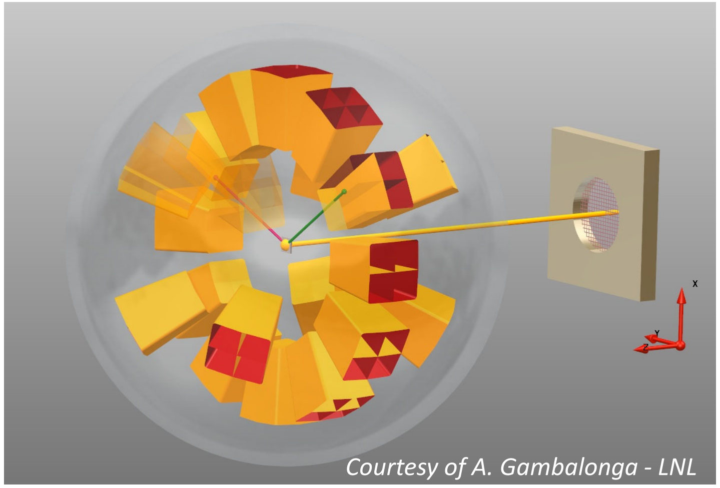

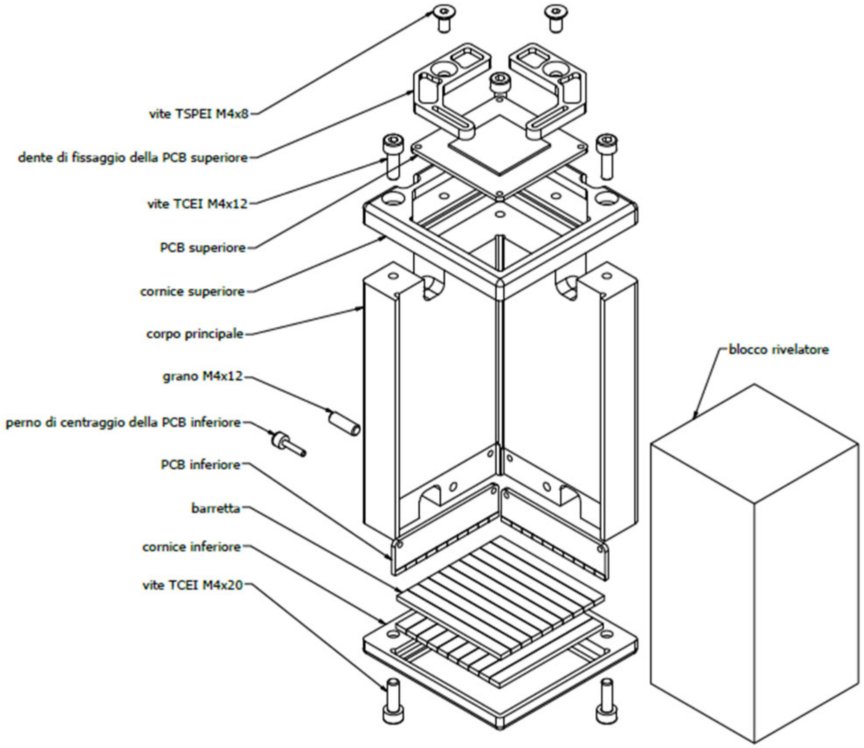

Design of the new setup: background suppression

[R. Bolzonella, An experimental setup for detection of e+e pairs in the decay of ^{8}Be, Università di Padova (2021)]

- Dominant **background source: γ-rays emission** from the populated resonances
- Request to select an event:
  - **coincidence in the 3 layers**
  - most of the ΔE is concentrated in a single bar or in the closest one
  - energy cuts in the ΔE-E spectrum
  - γ detection efficiency in a single clover: ***ε = 6 · 10⁻⁴***
  - Detecting pairs:

$$R = \frac{N_{e^+e^-}}{N_{\gamma\gamma}} = \frac{\epsilon_l^2}{\epsilon_\gamma^2} \cdot \beta \quad \longrightarrow \quad R \sim 10$$

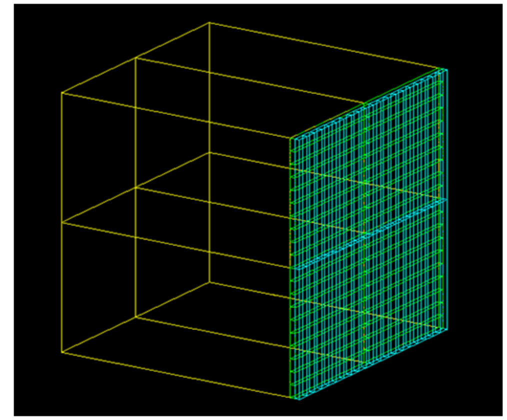

1 block – GEANT4 simulation

ΔE-E correlation

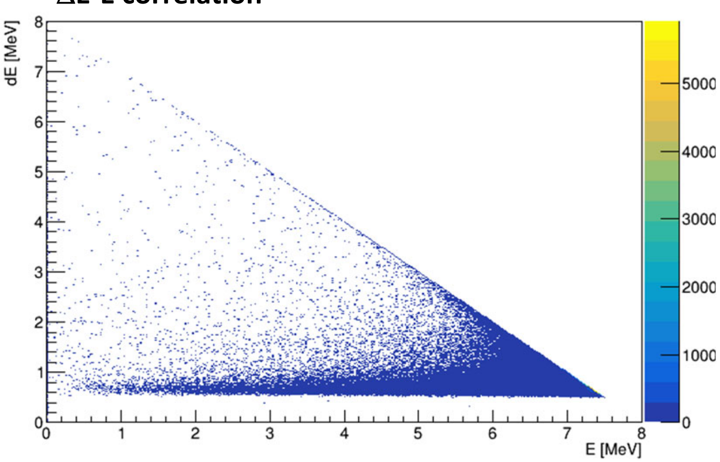

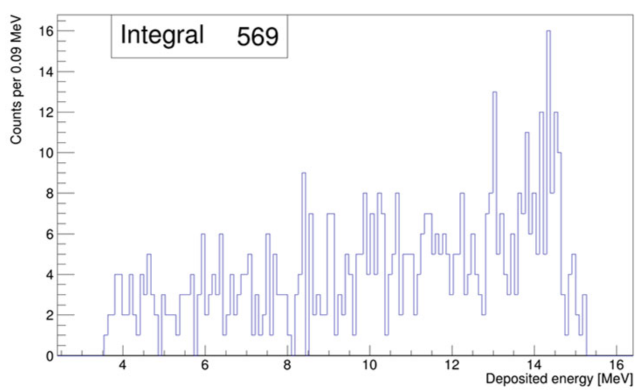

Energy spectrum for one block gated on triple coincidence (10^6 sim events)

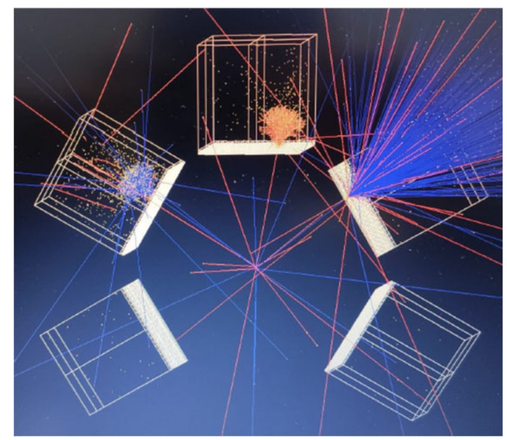

One possible configuration

Pair detection efficiency: two angular configurations

A – Angles: 0° - 60° - 120° - 180° - 270° (Atomki configuration)

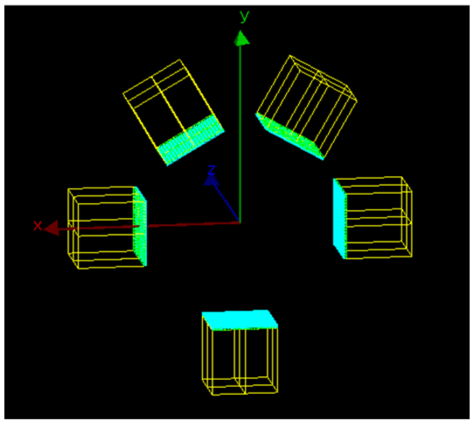

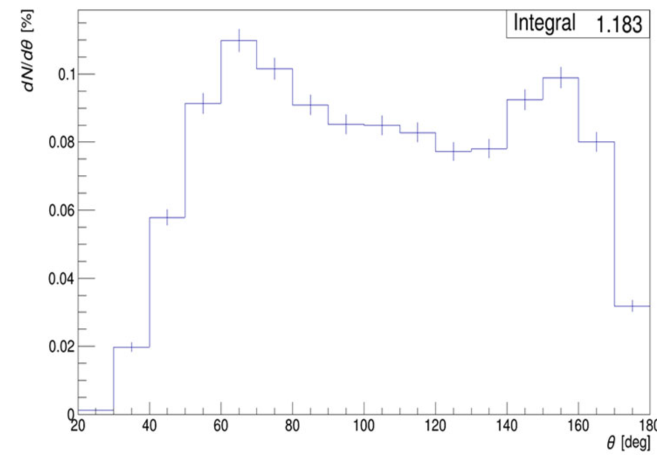

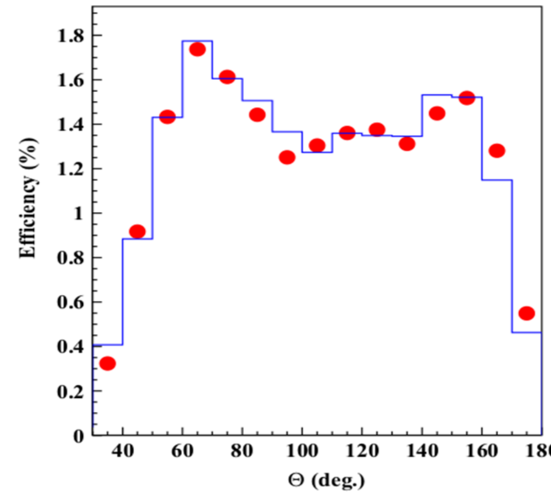

Good compatibility in shape with respect to the Atomki configuration. [J. Gulyás et al, NIM A 808, 21 (2016)]

B – Angles: 0° - 45° - 105° - 155° - 245°

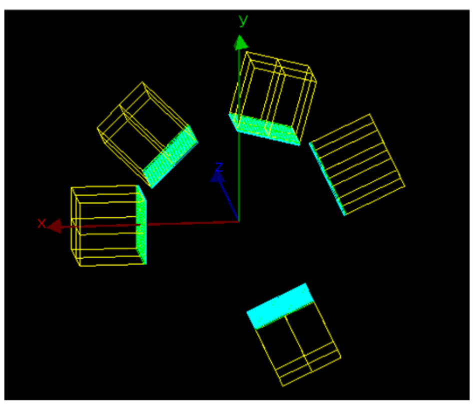

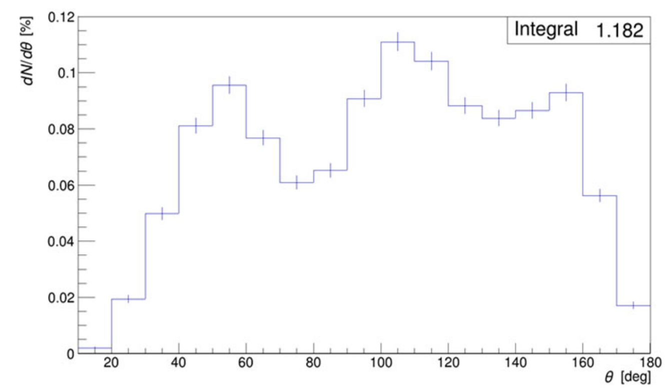

Estimated Pairs detection efficiency

ε_{pairs} = 1.18 %

The new setup: prototypes

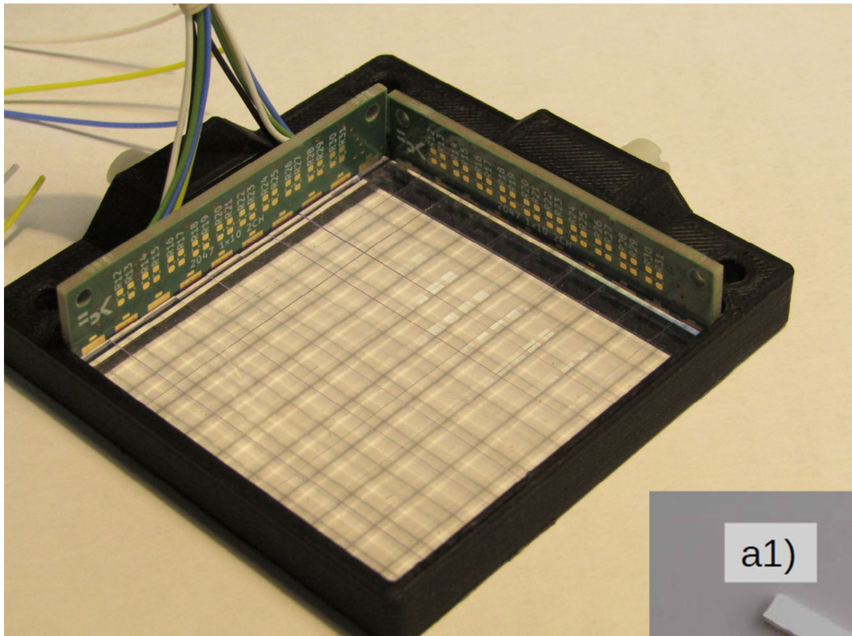

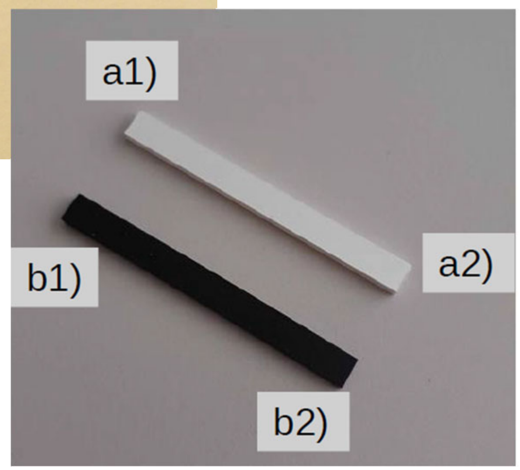

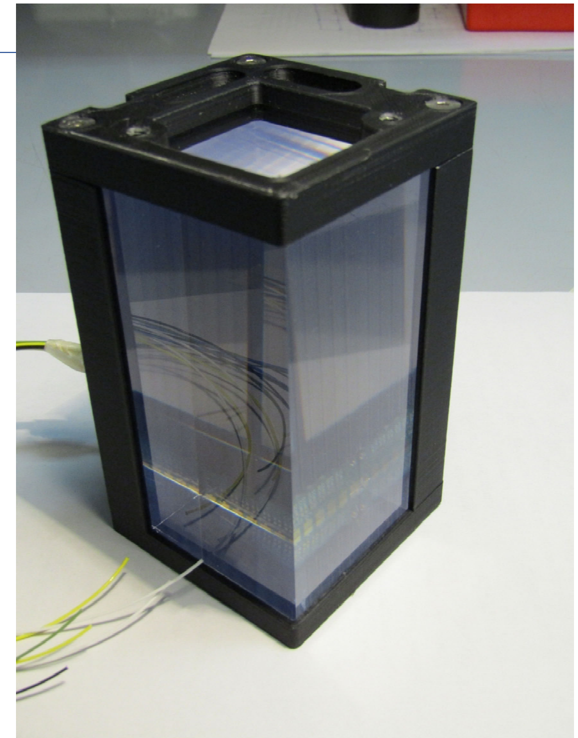

Experimental setup

- Bars read with an array of 10 SiPMs
- Signal of each SiPM distributed at the two extremes of the array using LG technology by FBK.
    - Total energy: $\boldsymbol{E_{TOT} = E_L + E_R}$
    - Energy asymmetry: $\boldsymbol{y} = \dfrac{E_R - E_L}{E_R + E_L}$

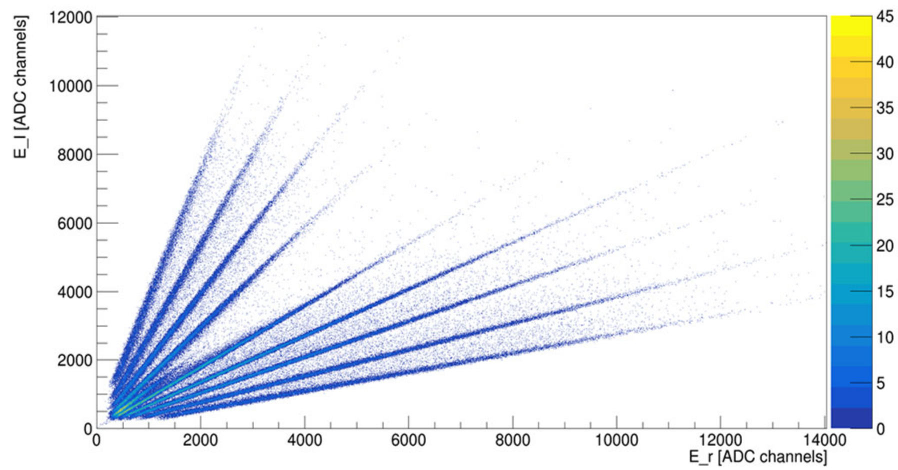

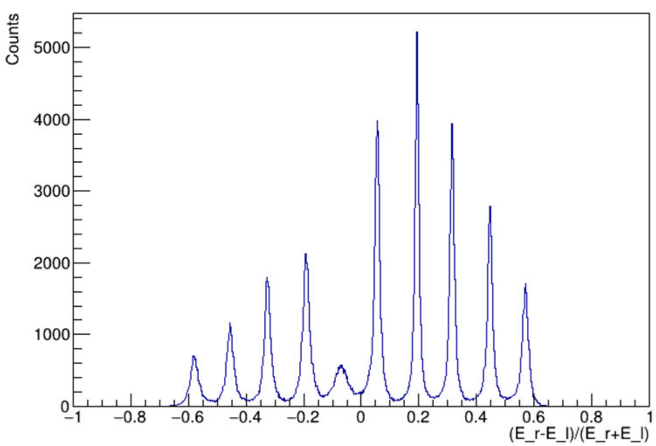

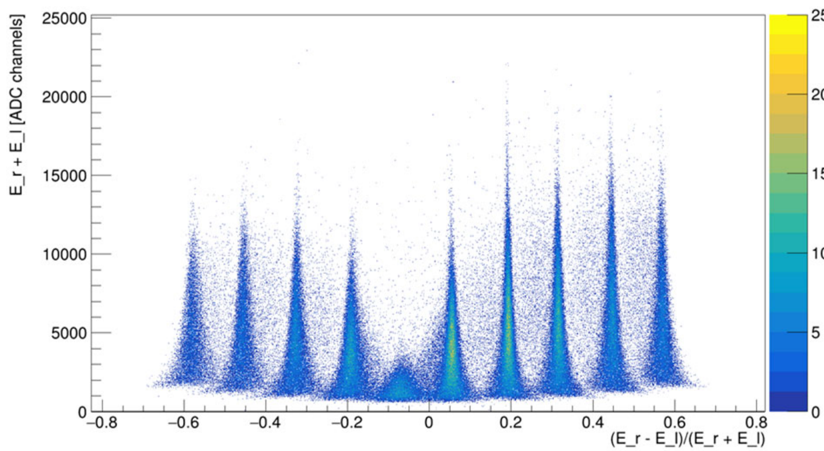

Calorimeter characterization: light yield estimate using Compton scattering

Setup:

- Source: ^{60}Co
- EJ200 detector read with SiPM FBK
- Ancillary detector: NaI(Tl) read with PMT
- Three light readout modes:
  - 1 SiPM (6x6 mm) -> 36 mm^2
  - 2 SiPMs (6x6 mm) -> 72 mm^2
  - 1 SiPM (10x10) -> 100 mm^2

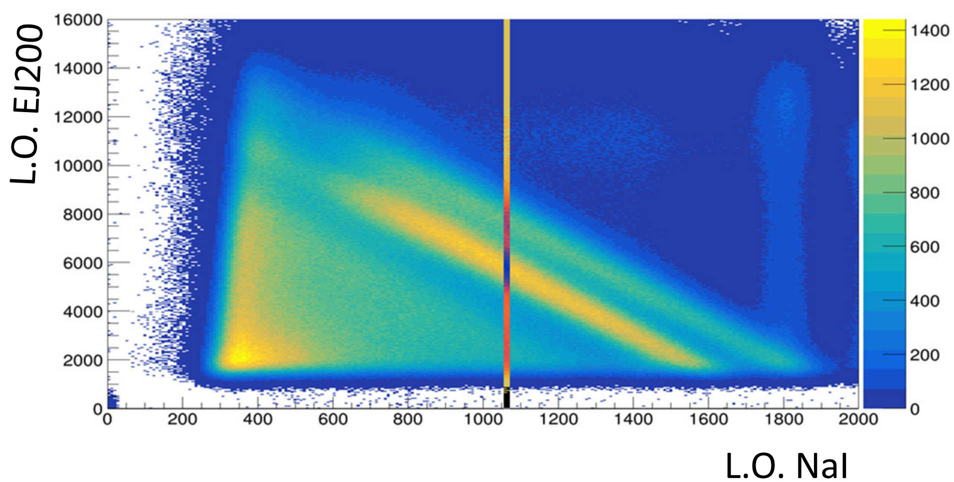

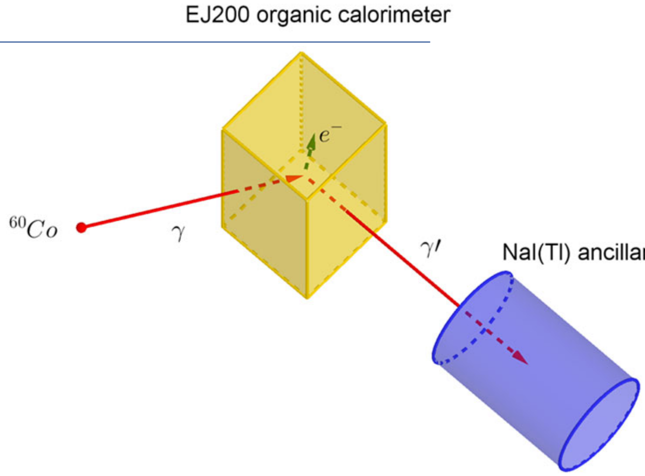

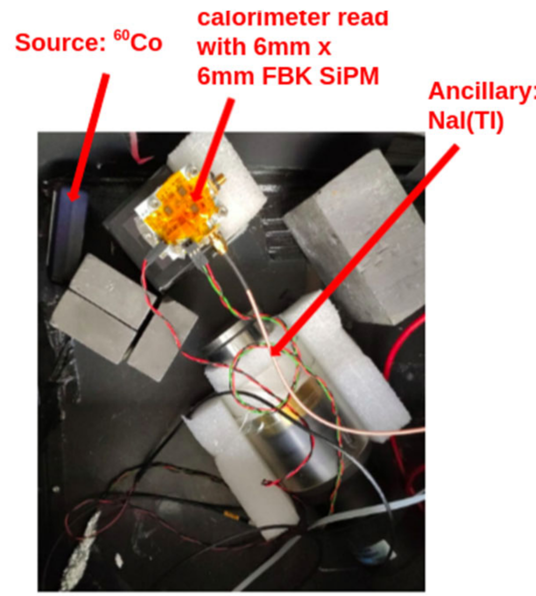

Calorimeter characterization: light yield estimate using Compton scattering

- **Slice** of the spectrum at fixed energy in the ancillary detector
- Energy in the organic scintillator fixed for energy conservation
- Projecting the slice in the organic scintillator energy measured, **pseudo-photopeaks** are produced
- Repeating the analysis for several energies, a **linear trend** in the plot of $1/R^2$ against the energy is expected
- *Best case: (100mm2) $L_y = 237 \pm 5$ photons/MeV*

SIPM Surface	Light Yield ph/MeV
36 mm^2	35.5 ± 0.7
72 mm^2	120 ± 3
100 mm^2	237 ± 5

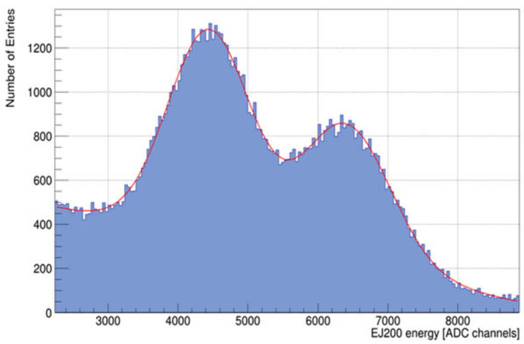

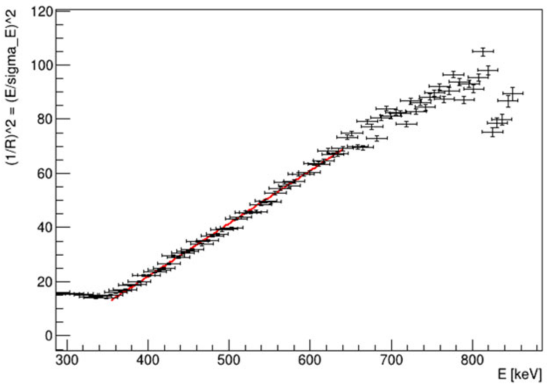

Invariant mass resolution estimate

- **Invariant mass** depends on:
  - e^- and e^+ energy
  - correlation angle
- The associated error depends on:
  - e^- energy (the e^+ one is fixed by the energy conservation)
  - energy resolution (depending on the light yield)
  - correlation angle
  - angular resolution
- Resolution computed as function of: $\mathbf{E^-}$, **Ly**, $\boldsymbol{\theta}$, $\boldsymbol{\sigma_\theta}$
- Electron energy and correlation angle integrated out

Invariant mass resolution

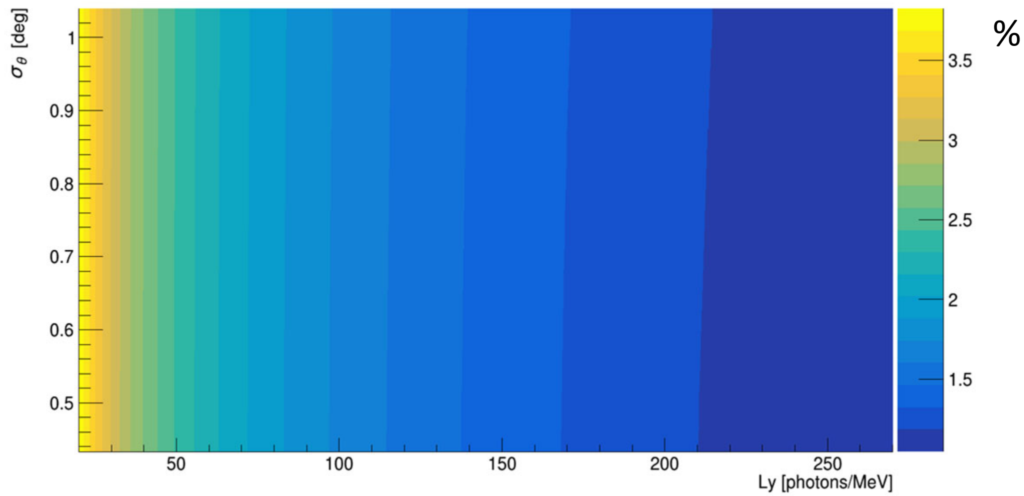

Upgraded and engineered tracking layers

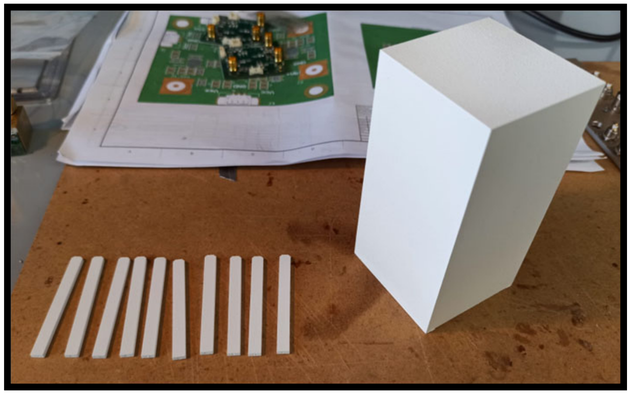

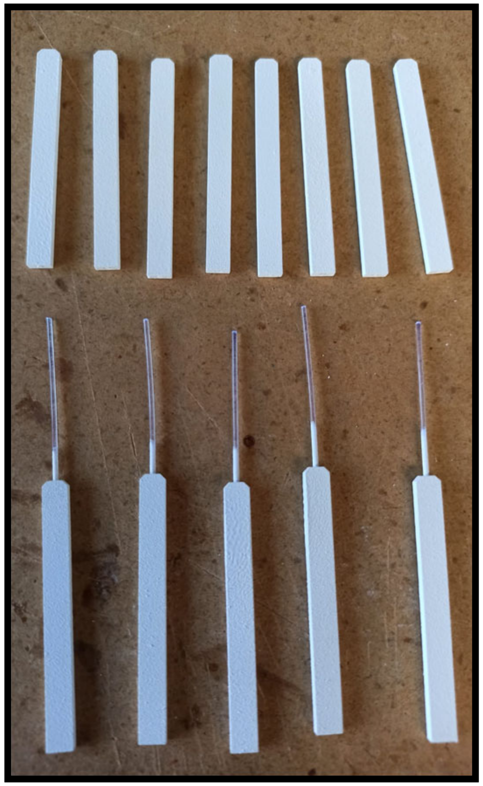

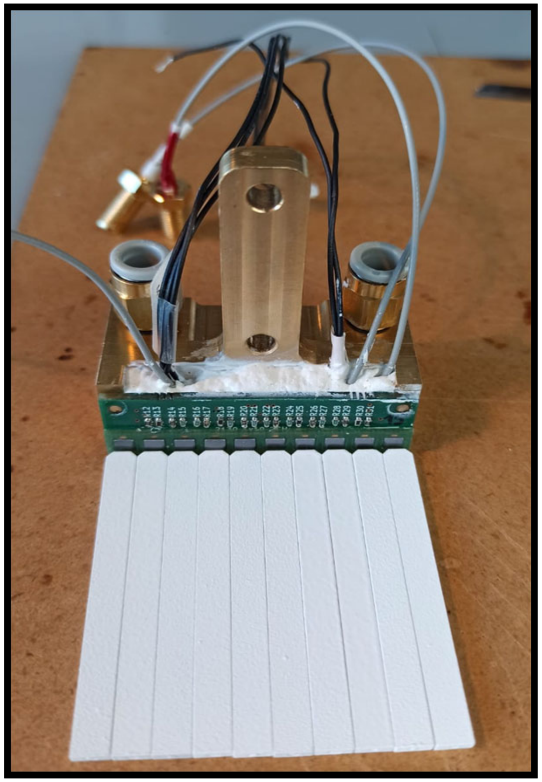

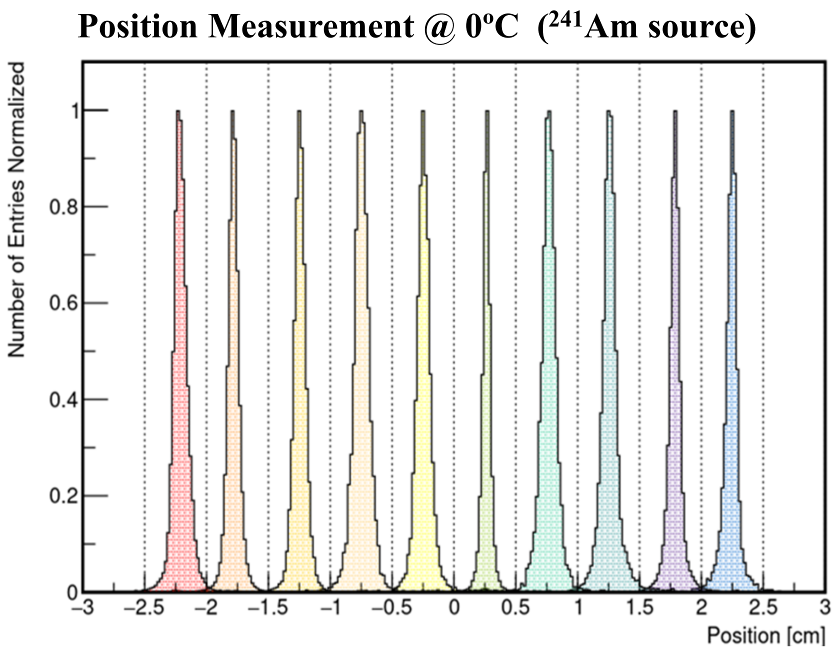

Positon:

$$x = \frac{E_r - E_l}{E_r + E_l}$$

E_l

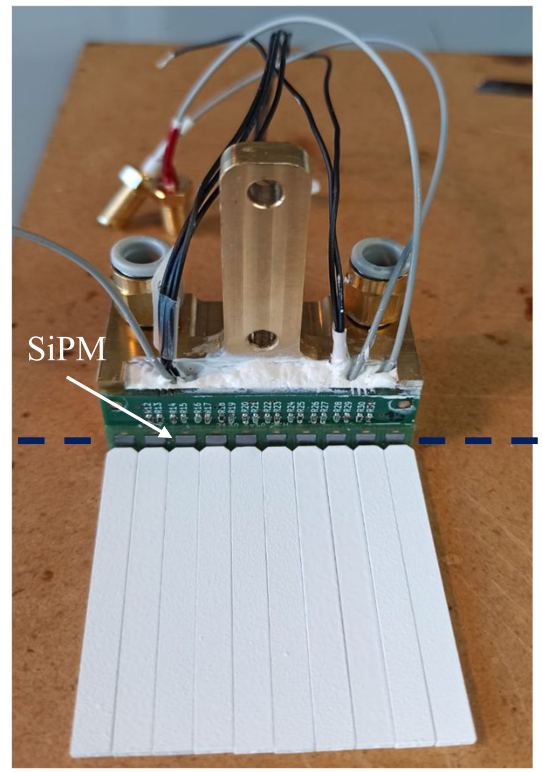

E_r

Deposited Energy:

$$E = E_r + E_l$$

Position Measurement @ 0ºC (^{90}Sr/ ^{90}Y source)

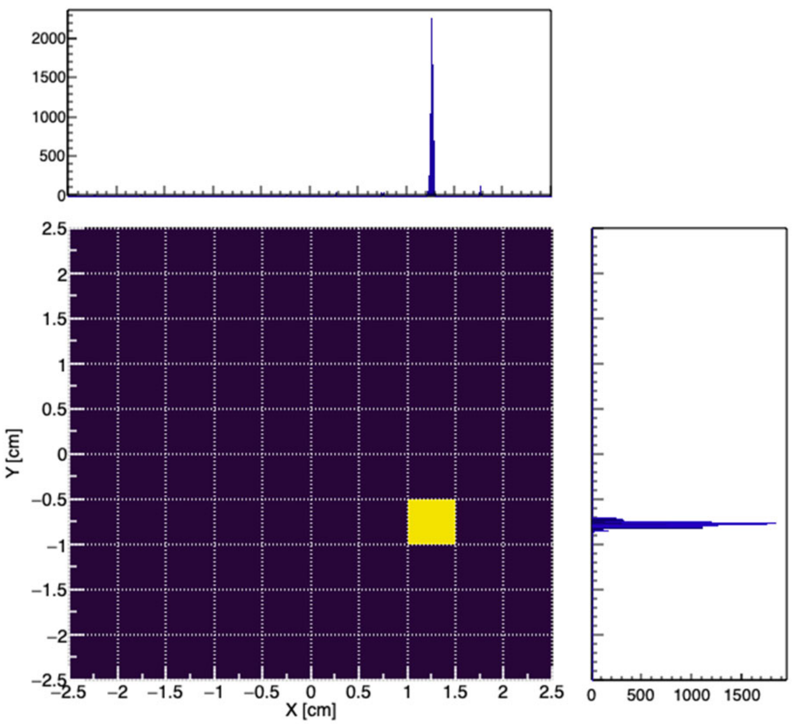

Positon:

$$x = \frac{E_r - E_l}{E_r + E_l}$$

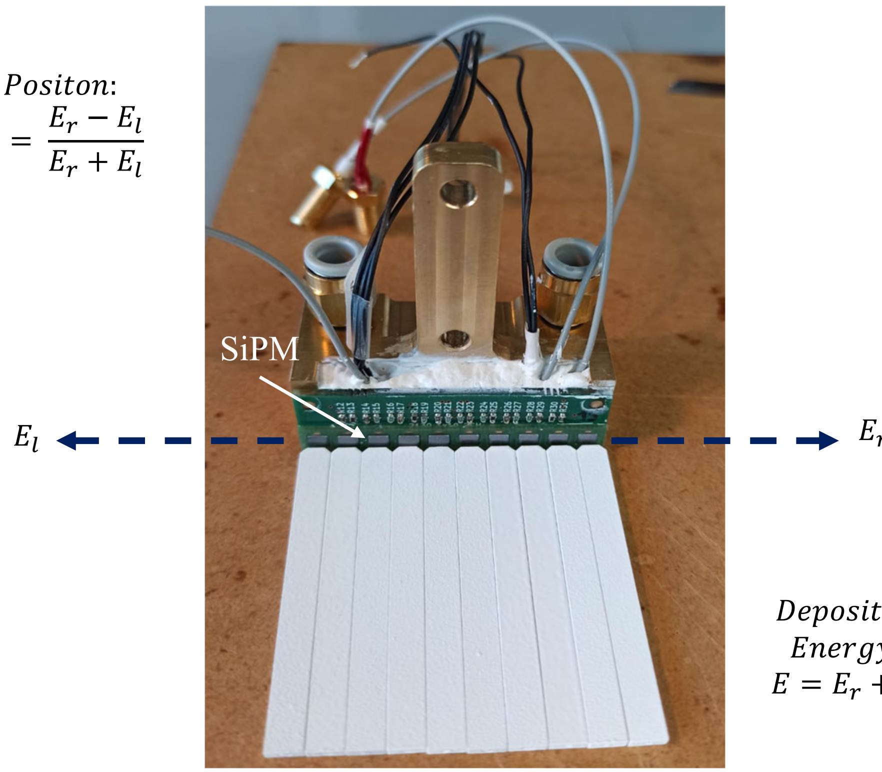

Deposited Energy:

$$E = E_r + E_l$$

Upgraded and engineered tracking layer’s characterization

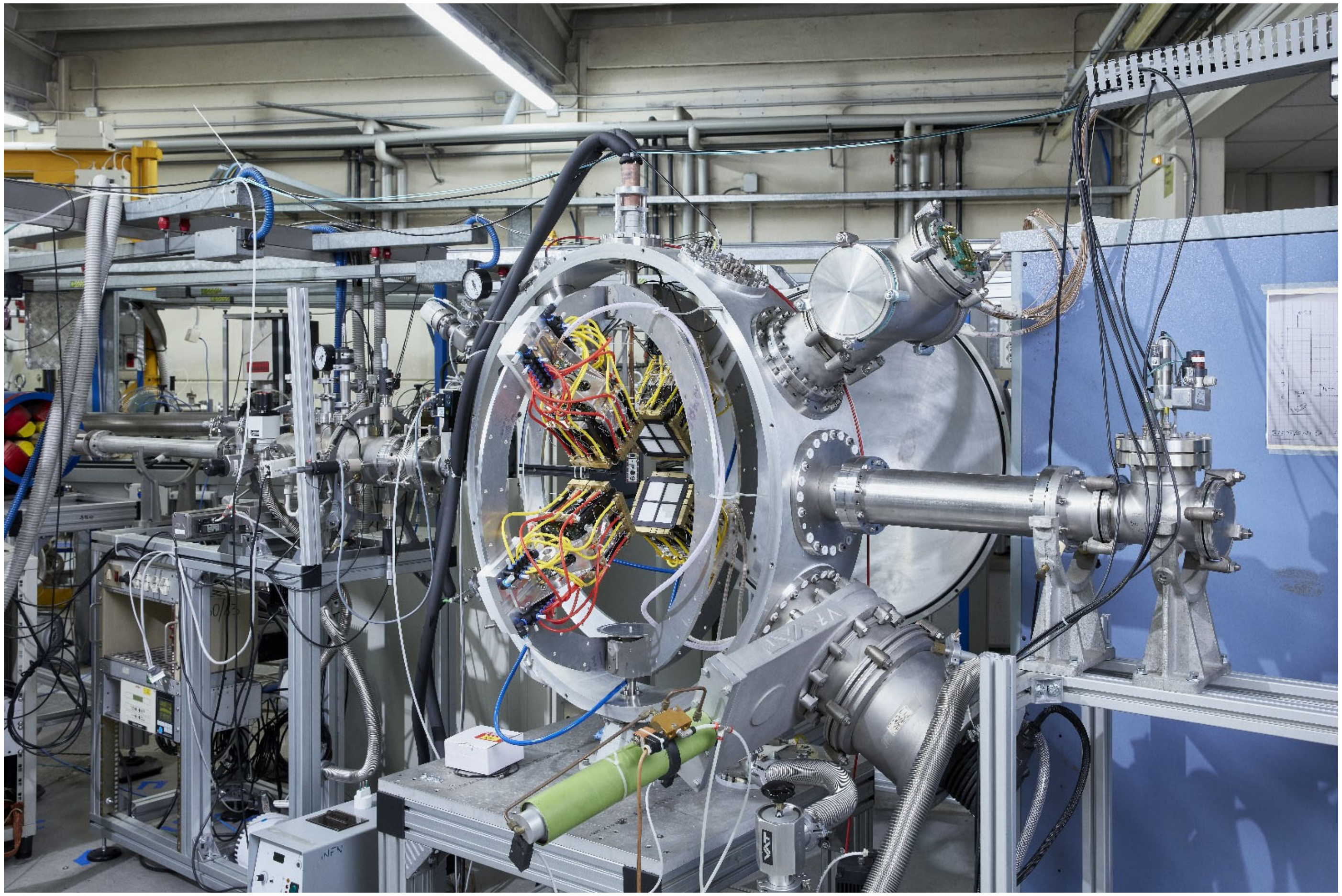

Setup @ AN2000 (30° beamline), LNL-INFN

- Cooling system based on antifreeze liquid (0°C).
- Block on top of the target ladder to cool the target frame.
- PT100 sensor to monitor the temperature in the detectors, target frame, and chamber
- Thermal camera to monitor the temperature in the target on the beam spot
- GRAFANA website to check in live time the temperature, vacuum levels, and beam current.
- System of two cameras for visual check of the target integrity

Setup @ AN2000 (30° beamline), LNL-INFN

- Cooling system based on antifreeze liquid.
- Block on top of the target ladder to cool the target frame.
- PT100 sensor to monitor the temperature in the detectors, target frame, and chamber
- Thermal camera to monitor the temperature in the target on the beam spot
- GRAFANA website to check in live time the temperature, vacuum levels, and beam current.
- System of two cameras for visual check of the target integrity

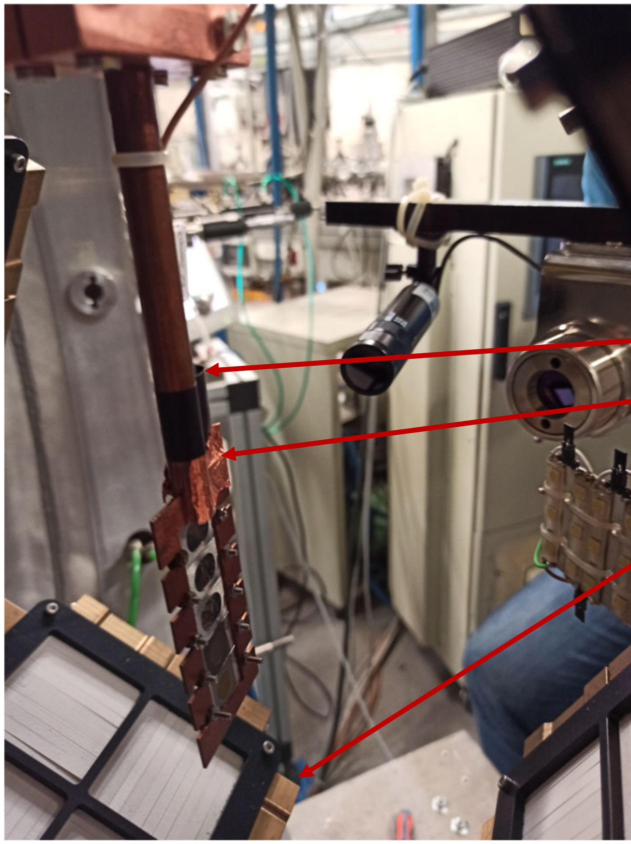

- Cooling system based on antifreeze liquid.
- Block on top of the target ladder to cool the target frame.
- PT100 sensor to monitor the temperature in the detectors, target frame, and chamber
- Thermal camera to monitor the temperature in the target on the beam spot
- GRAFANA website to check in live time the temperature, vacuum levels, and beam current.
- System of two cameras for visual check of the target integrity

Setup @ AN2000 (30° beamline), LNL-INFN

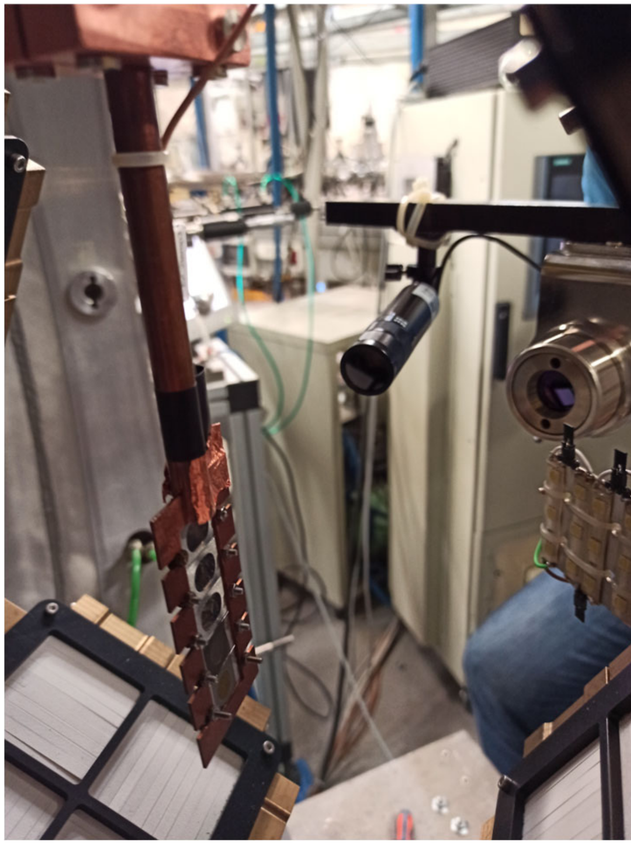

- Cooling system based on antifreeze liquid.
- Block on top of the target ladder to cool the target frame.
- PT100 sensor to monitor the temperature in the detectors, target frame, and chamber
- Thermal camera to monitor the temperature in the target on the beam spot
- GRAFANA website to check in live time the temperature, vacuum levels, and beam current.
- System of two cameras for visual check of the target integrity

Setup @ AN2000 (30° beamline), LNL-INFN – temperature monitoring

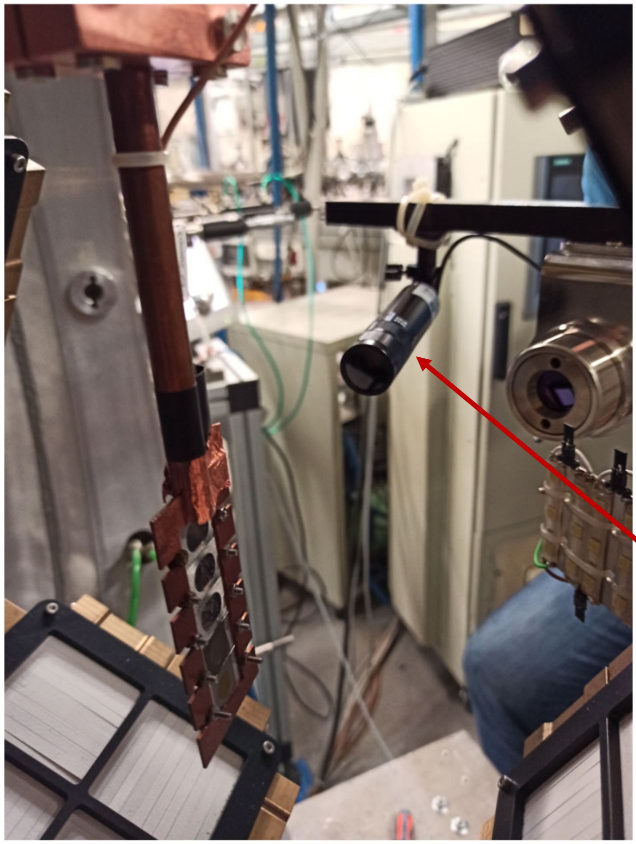

- Cooling system based on antifreeze liquid.
- Block on top of the target ladder to cold down the target frame.
- PT100 sensor to monitor the temperature in the detectors, target frame, and chamber
- Thermal camera to monitor the temperature in the target on the beam spot
- GRAFANA website to check in live time the temperature, vacuum levels, and beam current.
- System of two cameras for visual check of the target integrity

Setup @ AN2000 (30° beamline), LNL-INFN

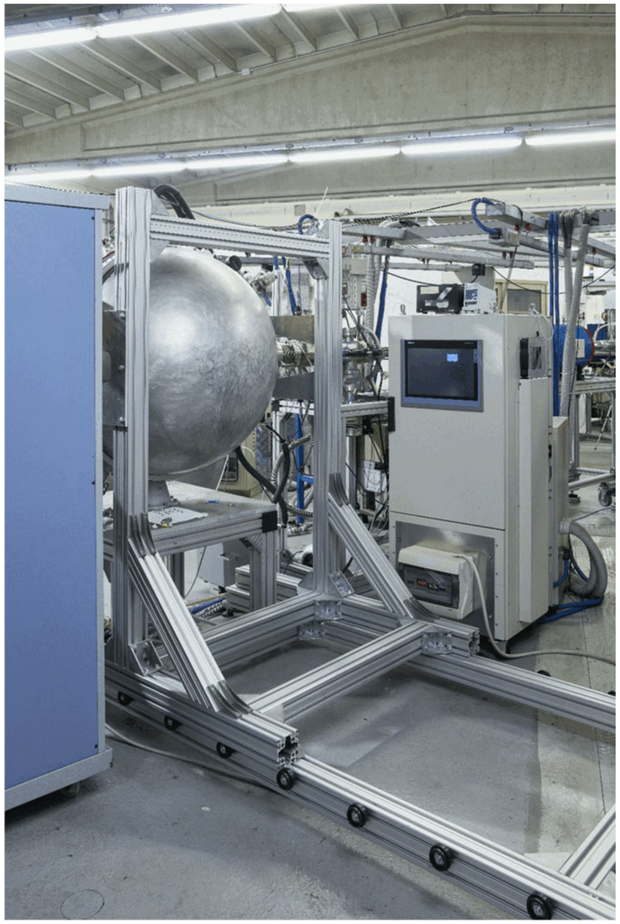

- In-beam test @ 451 keV proton beam: 5 days, 2 Clovers.
  - Target: LiF (80-950 μg/cm^2) on Cu backing (20-60 μg/cm^2)
- Isovector Magnetic Dipole Transition @ 445 keV proton beam: 9 days, 4 Clovers.
  - Target: LiF (30-100 μg/cm^2) on Cu and C backing (30-90 μg/cm^2)
- Isoscalar Magnetic Dipole Transition @ 1.03 MeV proton beam: 18 days, 4 Clovers.
  - Target: LiF (30-40 μg/cm^2) on C backing (20-50 μg/cm^2)

- $LaBr_3$ Detector to monitor the target
- Nuclear reactions of interest:
  - $^{19}F(p, \alpha e^{+}e^{-})^{16}O$
  - $^{7}Li(p, e^{+}e^{-})\,^{8}Be$

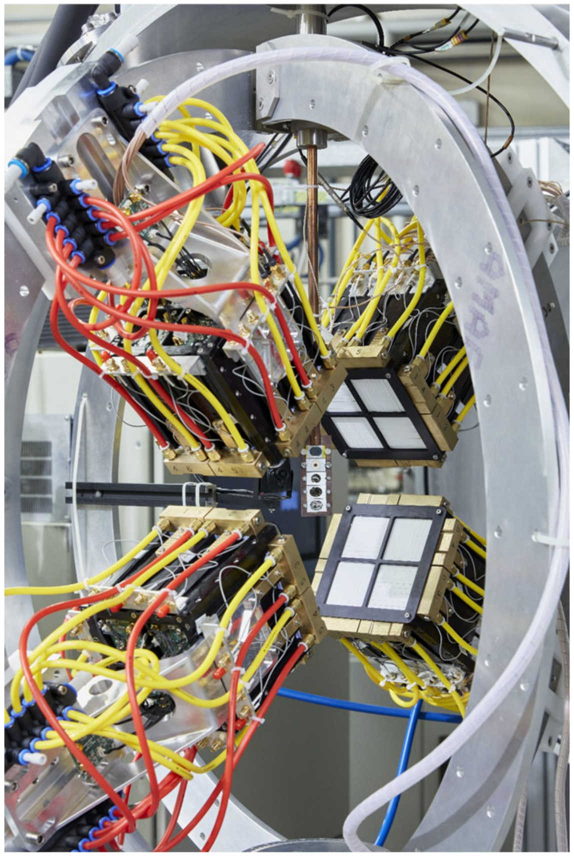

Sampling the excitation function

The $S(E)$ factor of $^7Li(p,\gamma)^8Be$ and consequences for $S(E)$ extrapolation in $^7Be(p,\gamma_0)^8B$

D. Zahnow[1], C. Angulo[2], C. Rolfs[3], S. Schmidt[1], W.H. Schulte[1], E. Somorjai[3]

[1]Institut für Physik mit Ionenstrahlen, Ruhr-Universität Bochum, Universitätstrasse 150, D-44780 Bochum, Germany
[2]CSNSM, Orsay, France
[3]ATOMKI, Debrecen, Hungary

Received: 30 August 1994/Revised version: 19 October 1994

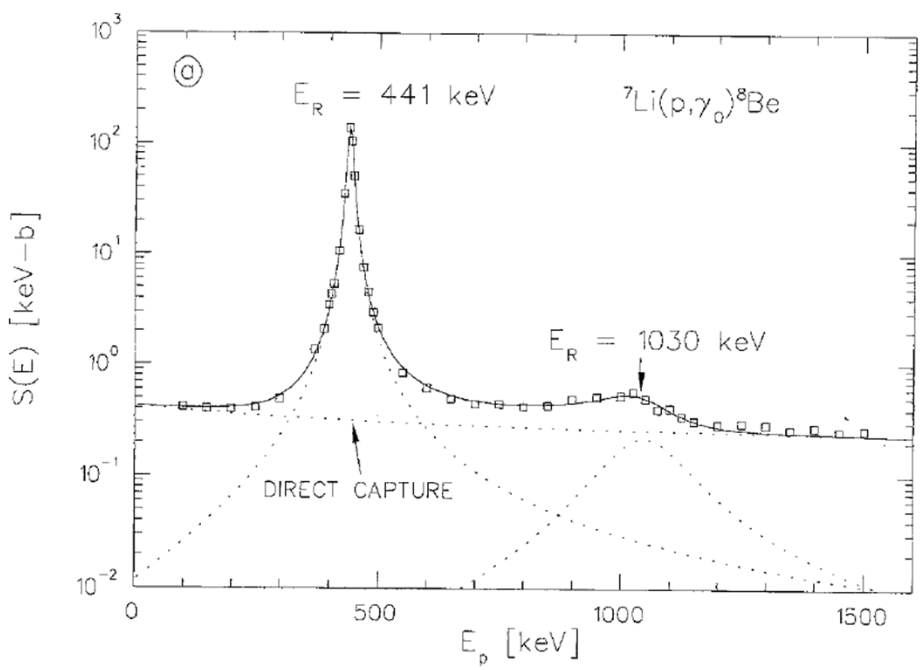

New analysis of $p+{}^{19}F$ reactions at low energies and the spectroscopy of natural-parity states in ^{20}Ne

Ivano Lombardo, Daniele Dell'Aquila, Jian-Jun He, Giulio Spadaccini, and Mariano Vigilante
Phys. Rev. C **100**, 044307 – Published 10 October 2019

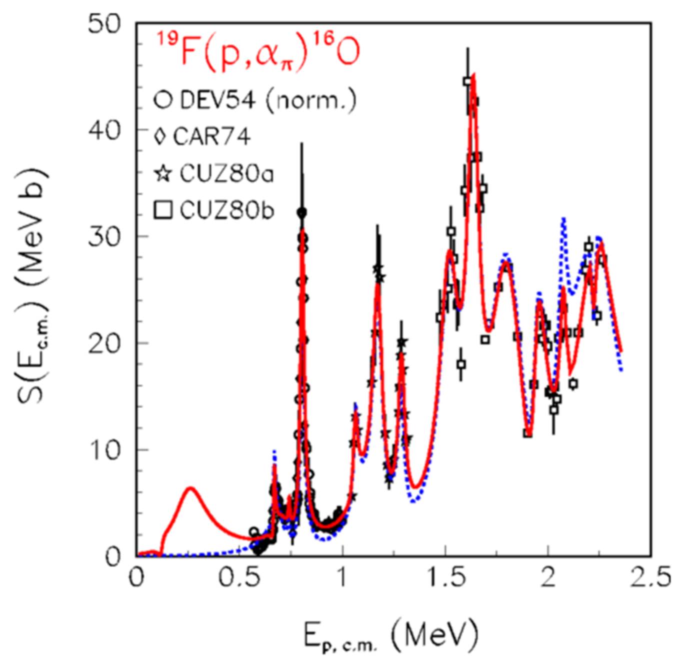

Beam and targets - gamma-ray Energy Spectrum (LaBr3) @ 441 keV

$LaBr_3$ spectrum for target monitoring and AN2000 calibration

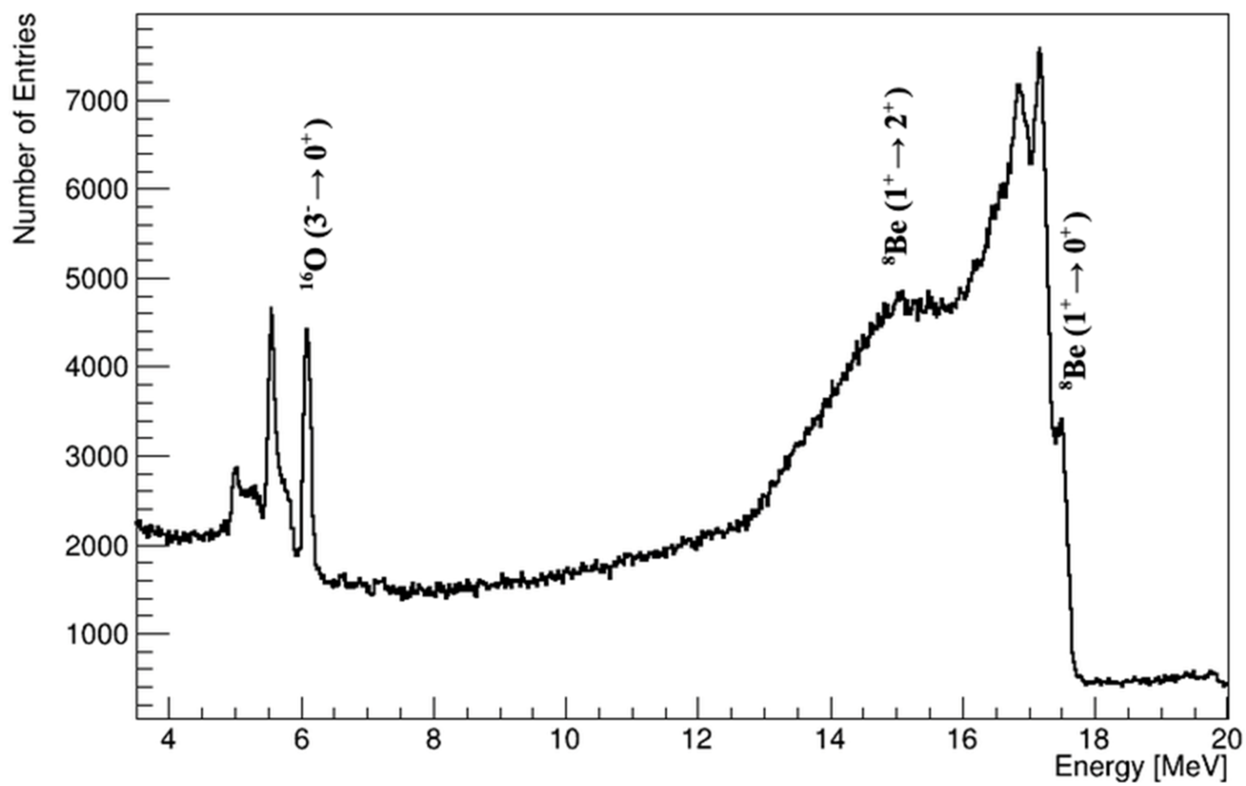

Beam and targets

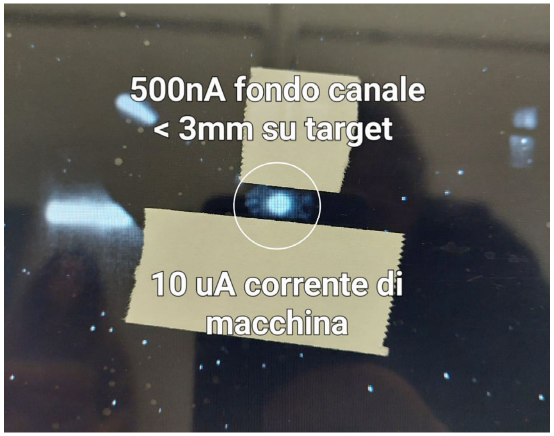

- H beam at 0.441 and 1.03 MeV (up to 600 nA)
- LiF on Cu backing
- LiF on C backing
- LiF with Au coating

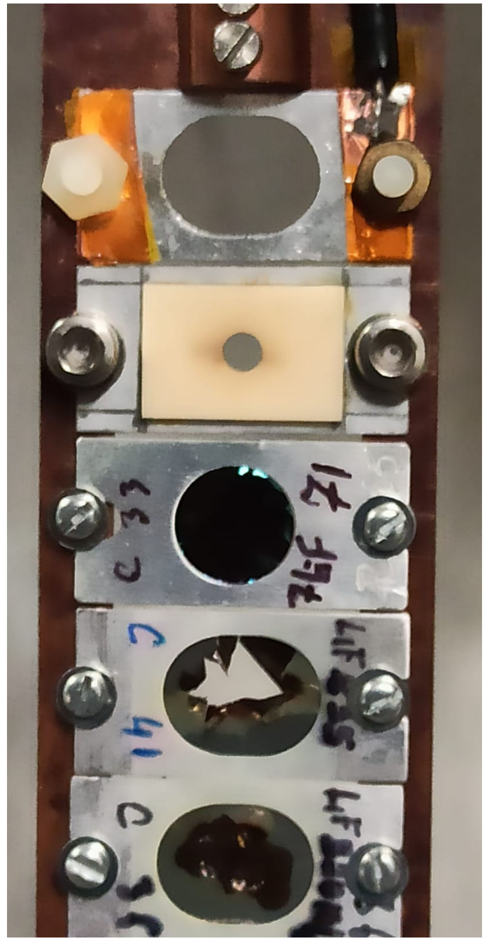

Preliminary results - on-line position reconstruction

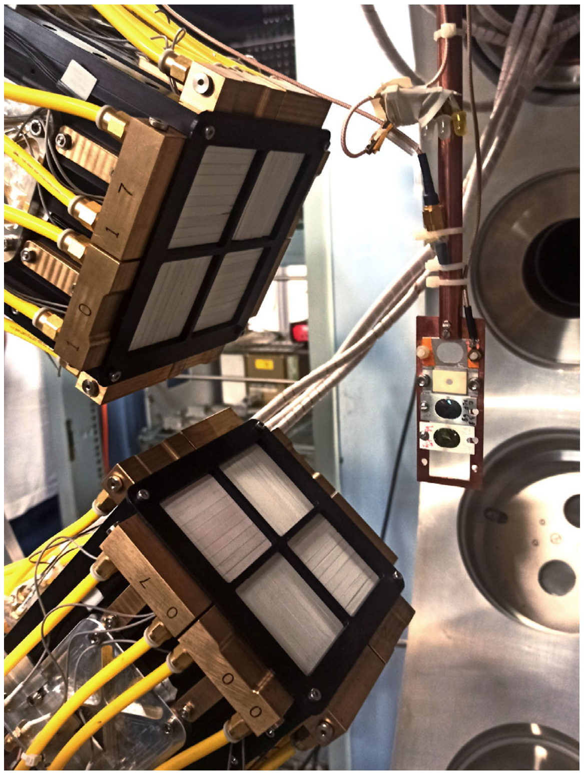

SiPM cooled at 0°C

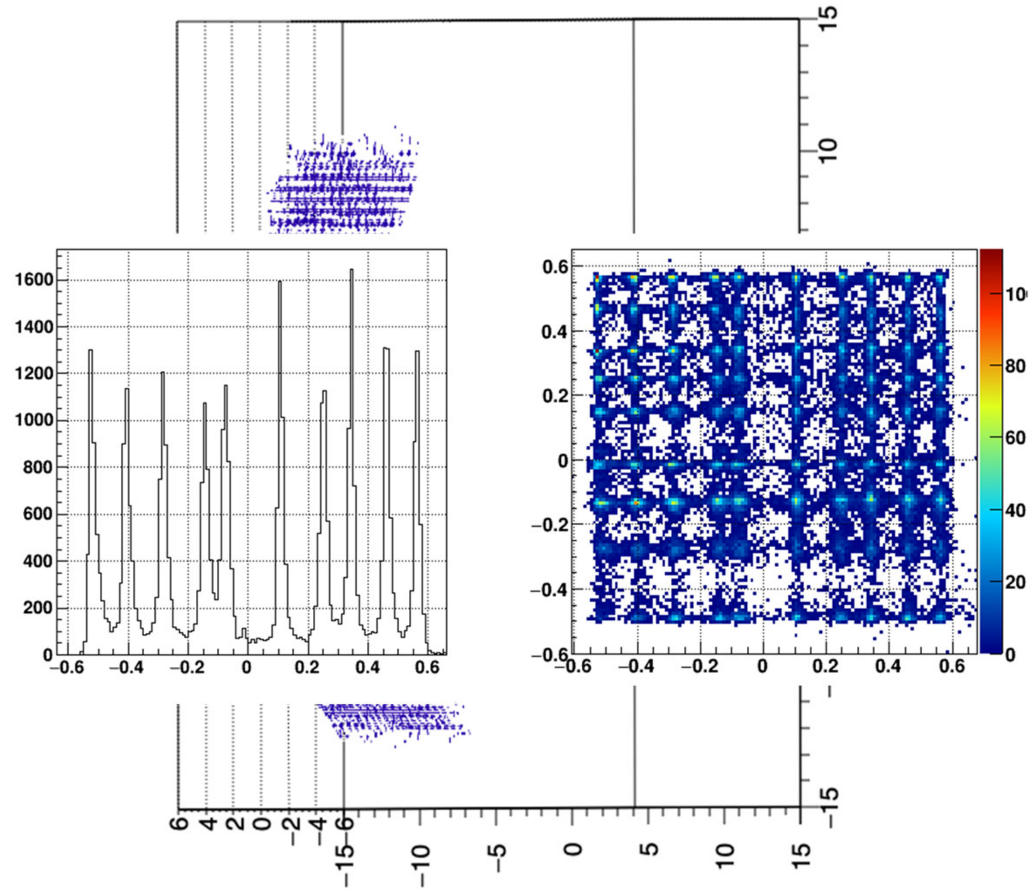

Preliminary results – correlation energy

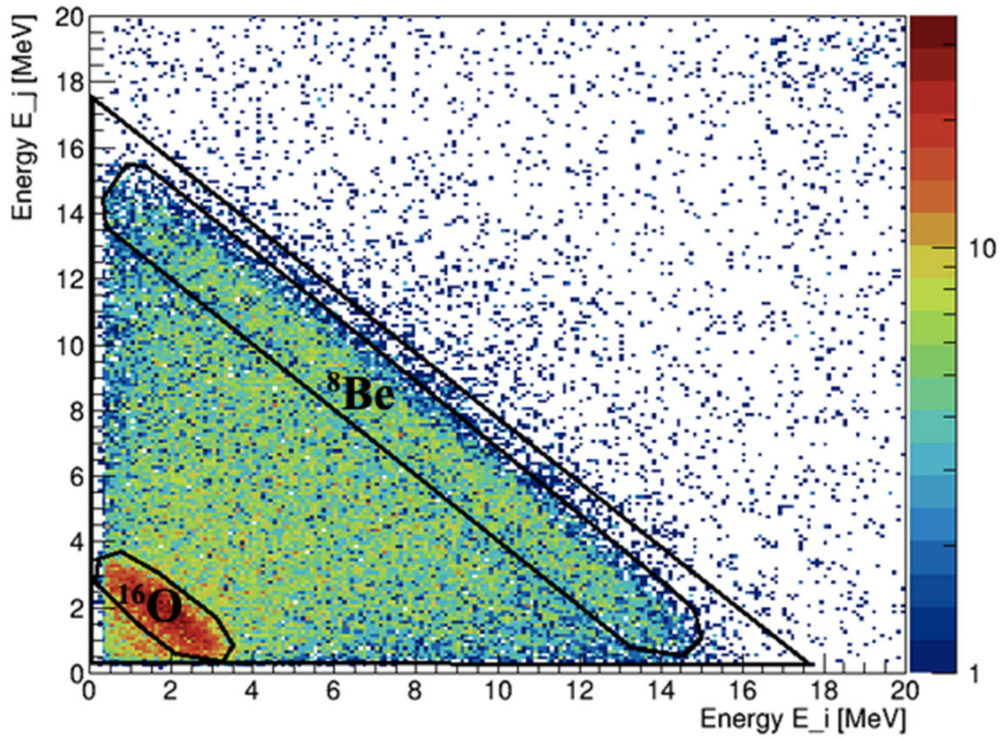

Preliminary results – energy asymmetry

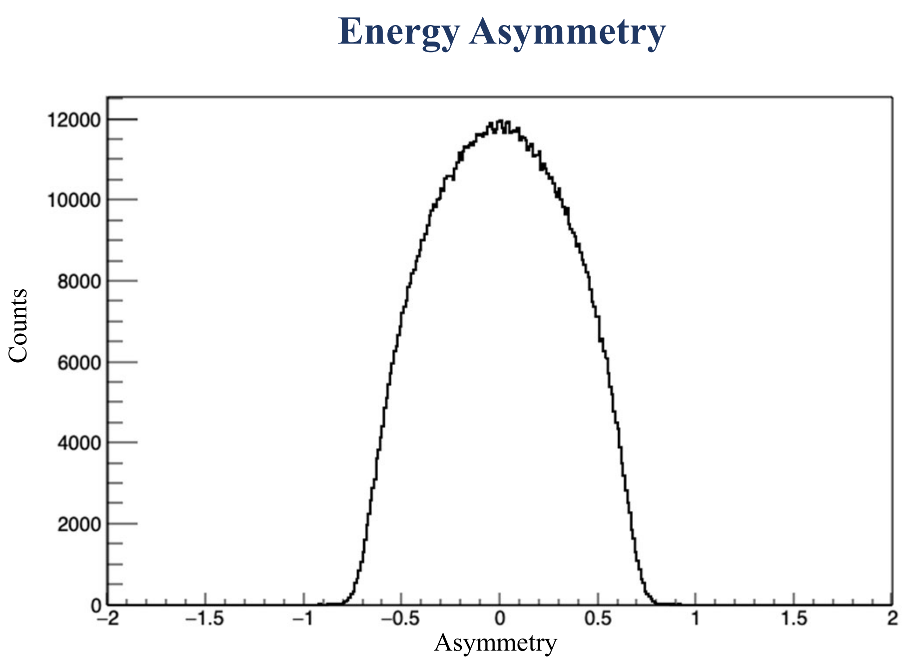

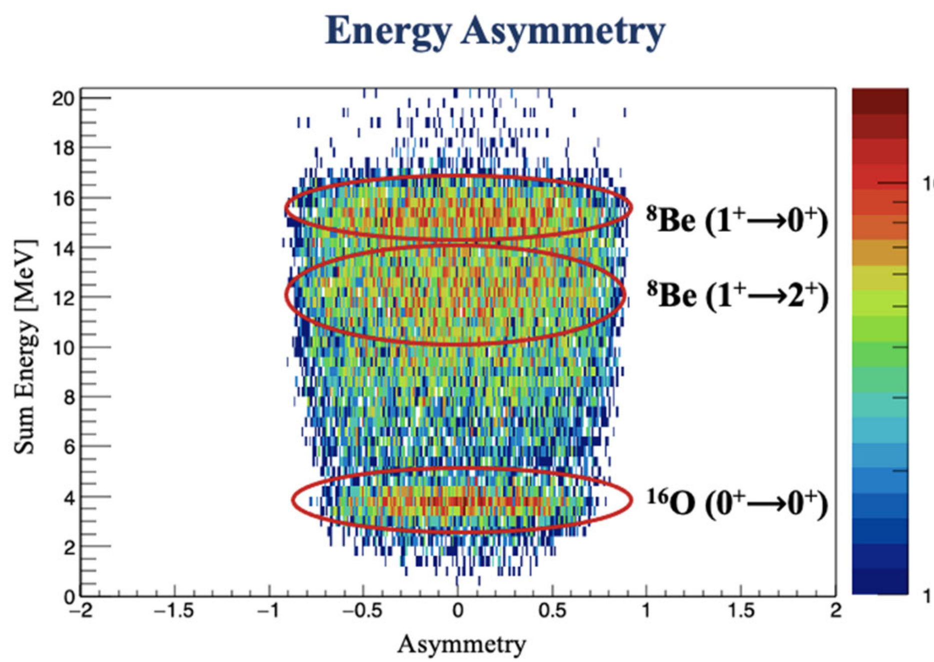

$\Delta E - E$

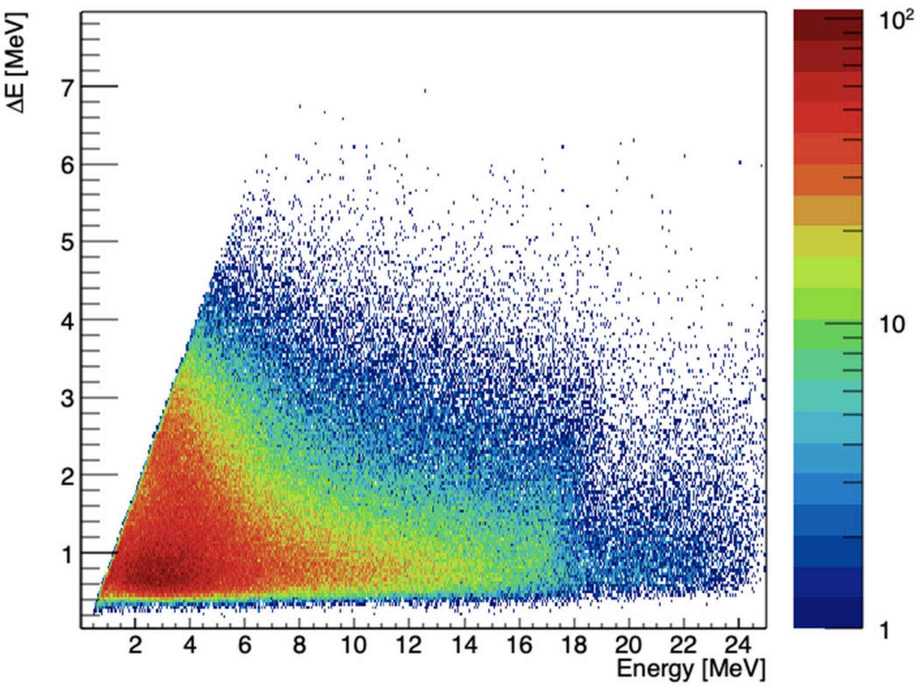

$\Delta E_{sum} - E_{sum}$

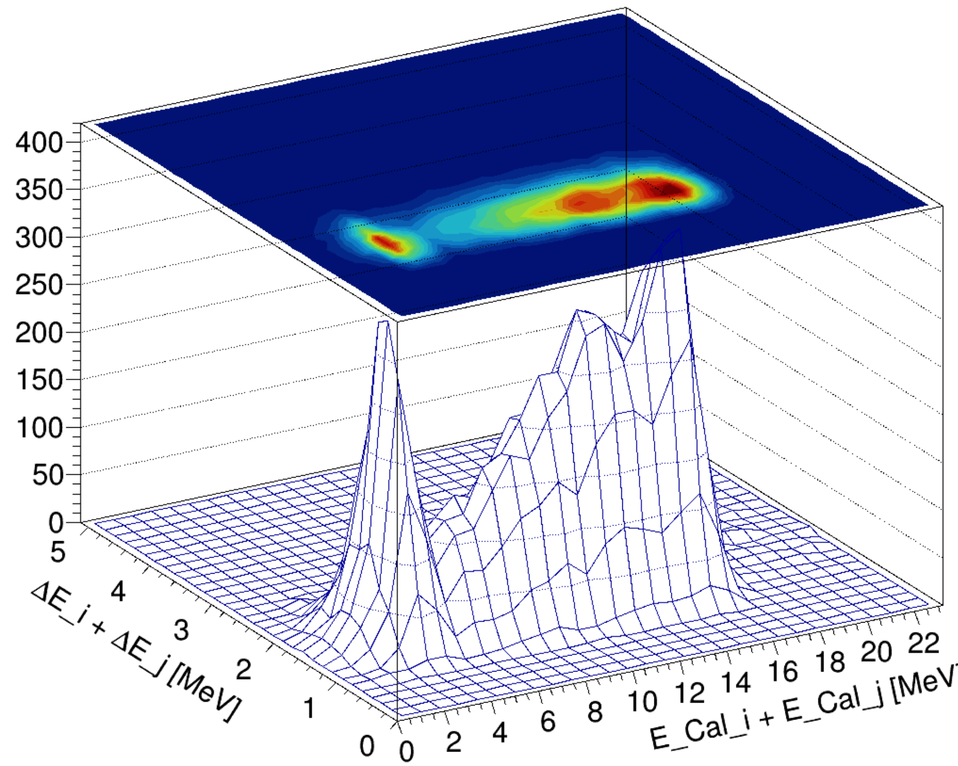

Preliminary results – reconstructed energy of the leptons @ 441 keV

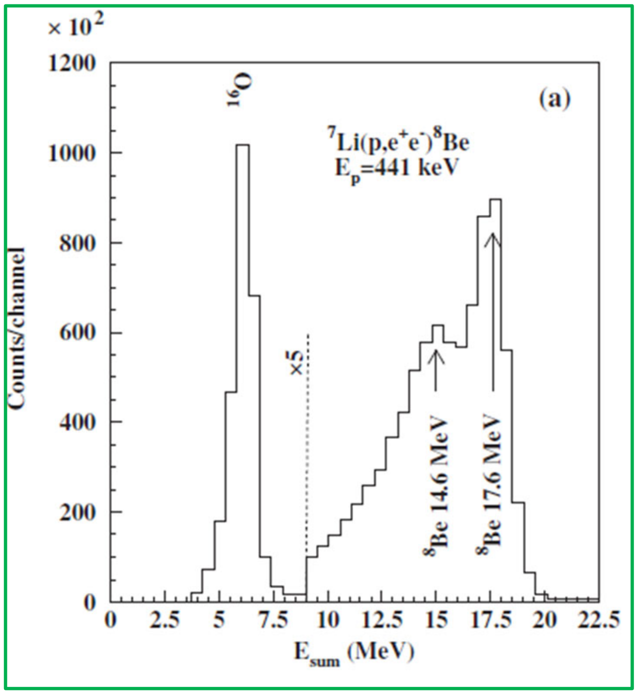

Reference

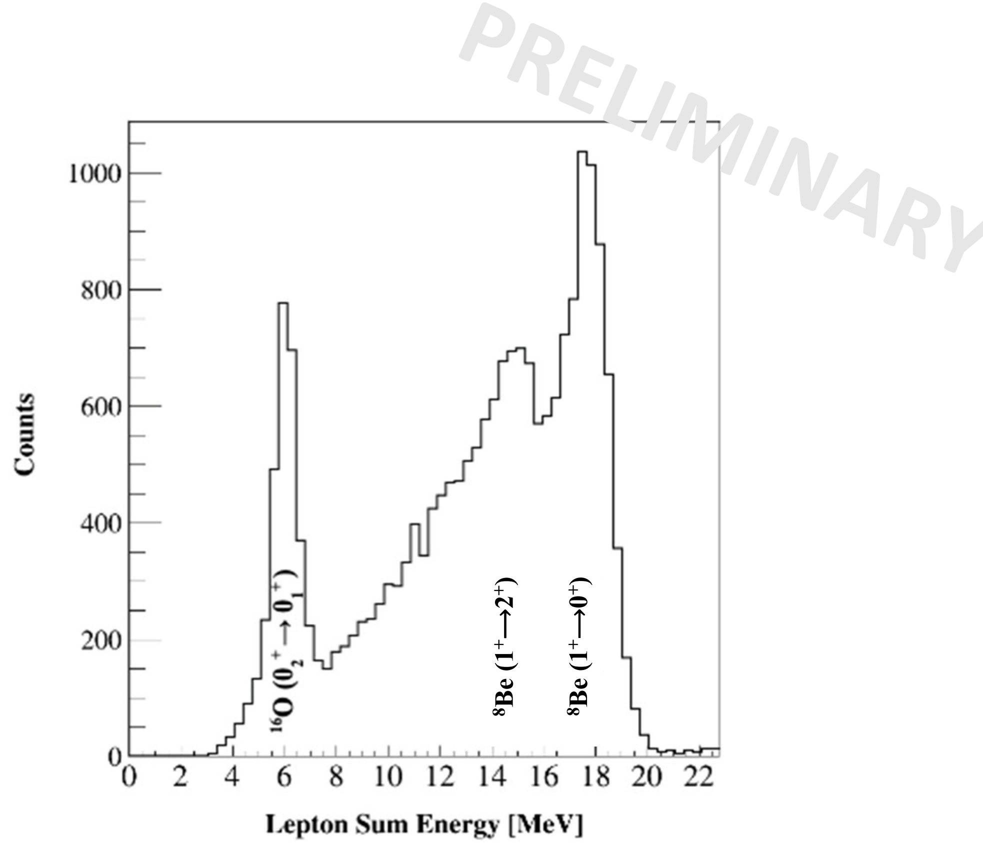

Measured

Preliminary results – reconstructed energy of the leptons @ 1050 keV

Beam energy / tgt thickness combination

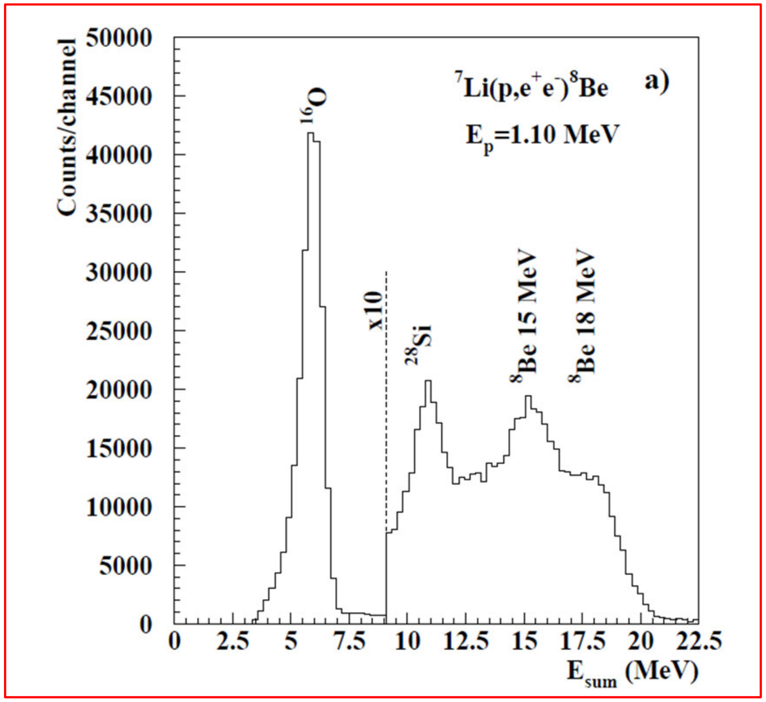

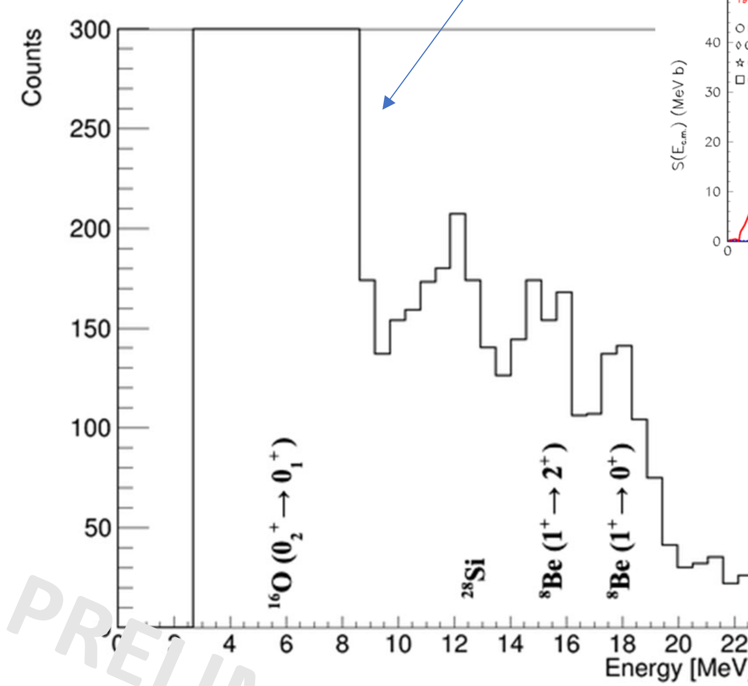

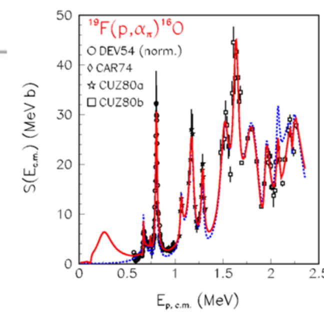

Preliminary results – uncorrected angular distribution ^{16}O

Geant4 Simulation

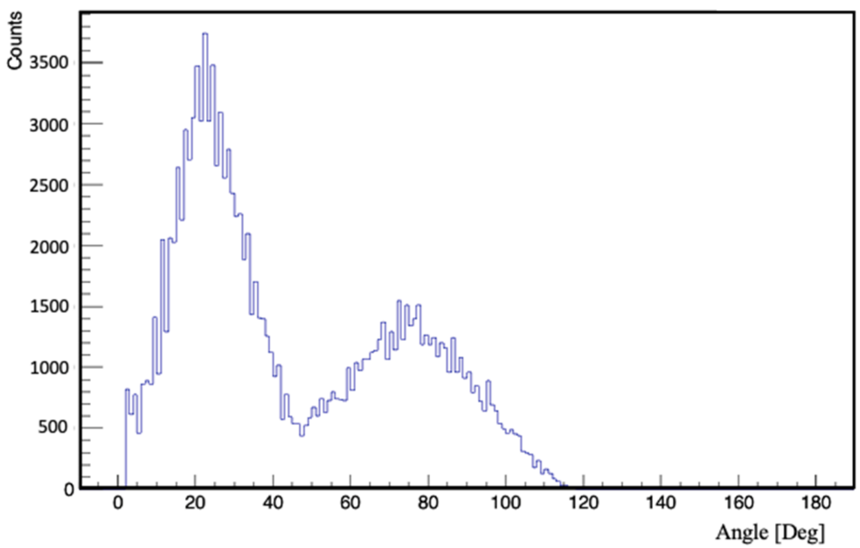

Commissioning data

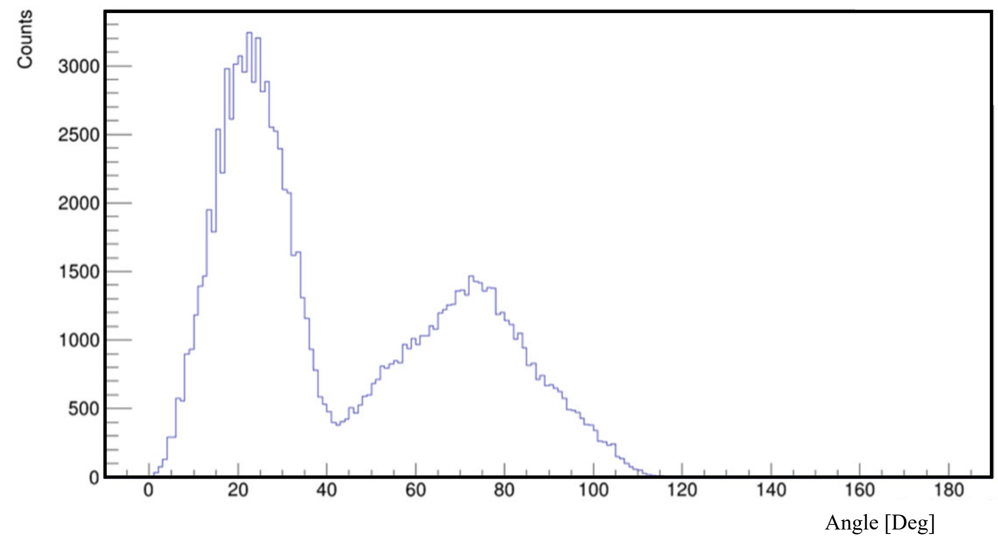

Outlook

$$\text{Protophobic vector boson: } \Gamma(^4\text{He}(20.21) \to {}^4\text{He}\,X) = (0.3 - 3.6) \times 10^{-5}\ \text{eV} \quad (126)$$

$$\text{ATOMKI Experiment [26, 27]: } \Gamma(^4\text{He}(20.21) \to {}^4\text{He}\,X) = (2.8 - 5.2) \times 10^{-5}\ \text{eV}. \quad (127)$$

The reported 7σ anomalies reported in ^8Be and ^4He nuclear decays are both kinematically and dynamically consistent with the production of a 17 MeV protophobic gauge boson.

What is the path forward? Clearly, now is the time for other collaborations to perform the same nuclear measurements to check the ATOMKI results. But in this work, we also propose simple modifications of the ATOMKI setup that could provide incisive tests of the new particle interpretation. The comparison between theory and experiment will be sharpened considerably by including the E1 background in the experimental analysis and running on the ^{4}He(20.21) 0^+ resonance. In addition, scanning through the ^{4}He(20.21) 0^+ resonance can provide important information to disentangle vector and axial vector X bosons and quantify the properties of particles with mixed couplings. Last, we find that the protophobic vector boson could also be observable in the decays of the ^{12}C(17.23) 1^- excited state, and we have provided precise predictions for this rate.

[J. L. Feng et al, Phys. Rev. D 102 (2020) 036016]

Outlook

TABLE I. Production and decay kinematic parameters. Beams of protons with kinetic energy E_{beam} collide with nuclei A at rest to form excited nuclei N_*, which then decay to the ground state nucleus N_0 through $N_* \to N_0 X$. We fix $m_X = 17$ MeV, and for each of the relevant processes, we give the values of E_{beam}, m_A, m_{N_*}, v_{N_*} (the N_* velocity in the lab frame), v_X (the X velocity in the N_* rest frame), and $\theta^{min}_{e^+e^-}$ (the minimum e^+e^- opening angle). ^{4}He(20.49) indicates the resonance energy probed in Ref. [33], which sits between the ^{4}He(21.01) and ^{4}He(20.21) states.

$p + A \to$	N_*	E_{beam} [MeV]	m_A [MeV]	m_{N_*} [MeV]	v_{N_*}/c	v_X/c	$\theta^{min}_{e^+e^-}$
$p + {}^7\text{Li} \to$	^{8}Be(18.15)	1.03	6533.83	7473.01	0.0059	0.350	139°
$p + {}^7\text{Li} \to$	^{8}Be(17.64)	0.45	6533.83	7472.50	0.0039	0.267	149°
$p + {}^{11}\text{B} \to$	^{12}C(17.23)	1.40	10252.54	11192.09	0.0046	0.163	161°
$p + {}^3\text{H} \to$	^{4}He(21.01)	1.59	2808.92	3748.39	0.0146	0.587	108°
$p + {}^3\text{H} \to$	^{4}He(20.49)	0.90	2808.92	3747.87	0.0110	0.557	112°
$p + {}^3\text{H} \to$	^{4}He(20.21)	0.52	2808.92	3747.59	0.0084	0.540	115°

[J. L. Feng et al, Phys. Rev. D 102 (2020) 036016]

Outlook: inverse kinematics and tracking. Nuclear decay tagging.

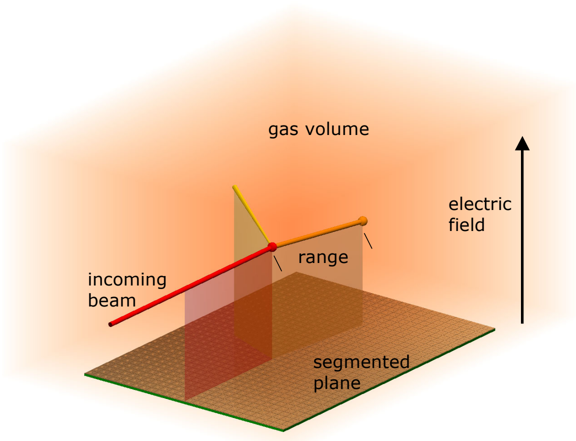

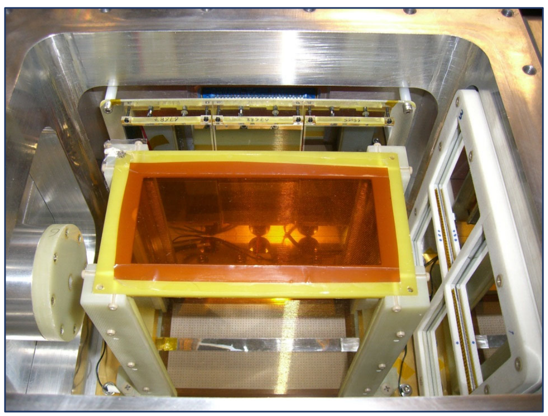

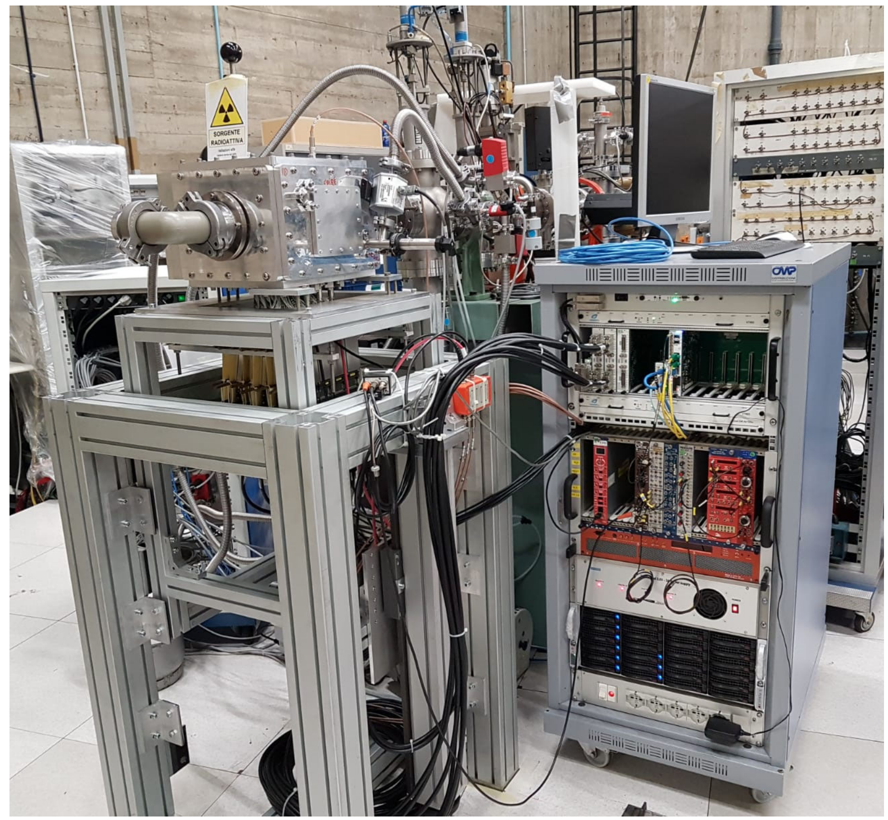

Outlook: inverse kinematics and tracking. Nuclear decay tagging.

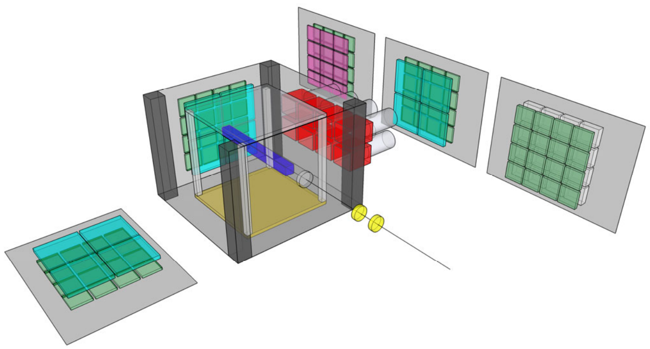

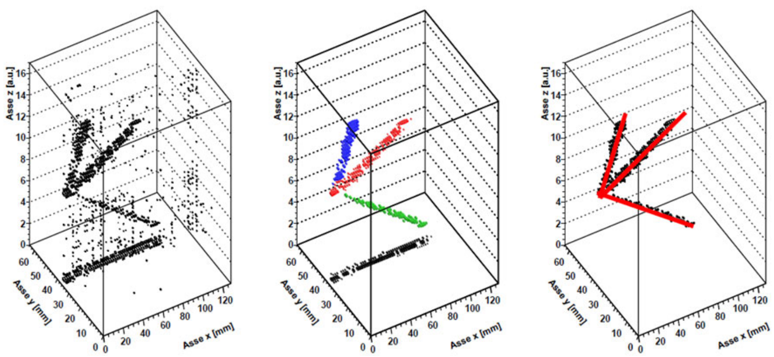

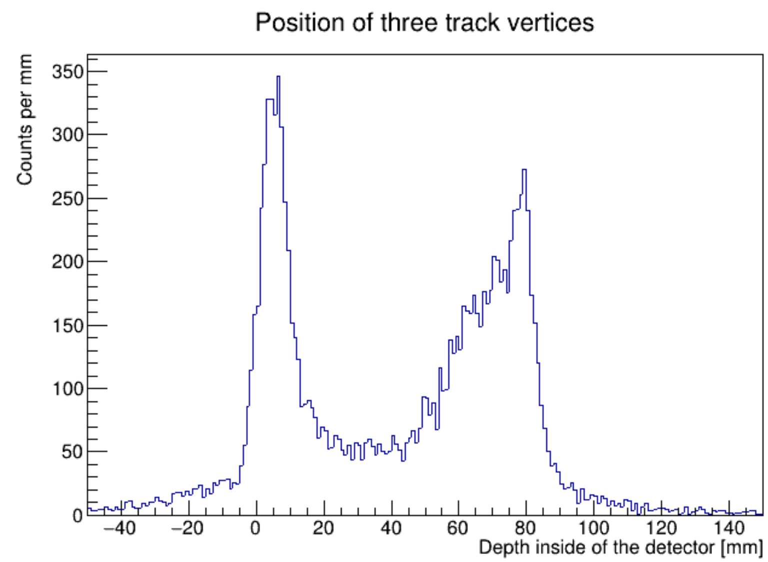

$^{11}B+iC_4H_{10}$ at 32 MeV

3 stopped particles in the output channel

Collaboration Members:

B. Gongora-Servin[1,2], T. Marchi[1], D. Tagnani[3], A. Goasduff[1], J.J. Valiente-Dobón[1], A. Celentano[5], F. Azaiez[1], P. Aguilera[4], F. Angelini[1,4], L. Baldesi[7], M. Balogh[1], S. Barlini[7], S. Bottoni[9], R. Bolzonella[2], D. Brugnara[1], J. Benito-Garcia[4], A. Camaiani[7], S. Carollo[4], G. Casini[7], G. Cobari[9], D. Dell'Aquila[6], F. Ercolano[7], A.Ertroprak[1], D. Fabris[4], F. Galtarossa[4], F. Gramegna[1], A. Gottardo[1], A, Gozzelino[1], D. Lazzaretto[4], I. Lombardo[6], D. Mengoni[4], A. Nannini[7], L. Palombini[4], J. Pellumaj[1,2], R.M. Perez-Vidal[1], S. Piantelli[7], S. Pigliapoco[4], M. Polettini[4], E. Pilotto[4], D. Stramaccioni[1,4], G. Spina[9], M. Sigmund F. Recchia[4], L. Redilogo[6], K. Rezynkina[4], L. Rigon[4], M. Rocchini[7], M. Rossi[4], M. Sedlak[1], F. Simpsi[4], S. Valdre[7], M. Vigilante[8], L. Zago[1,4], I. Zanon[10], L. Zappacosta[4].

[1]INFN Laboratori Nazionali di Legnaro, [2]Università di Ferrara , [3]INFN Sezione di Roma Tre, [4]Università di Padova e INFN Sezione di Padova, [5]INFN Sezione di Genova, [6]INFN Sezione di Catania, [7]Università di Firenze and INFN Sezione di Firenze, [8]INFN Università di Napoli Federico II e INFN Sezione di Napoli, [9]INFN Sezione di Milano, [10]Stockholm University, [11]RBI Zagreb